A&A manuscript no.
(will be inserted by hand later)

Your thesaurus codes are:
08 (08.06.3; 08.12.1; 08.23.1; 10.05.1; 10.06.1; 12.04.1)

ASTRONOMY AND ASTROPHYSICS
April 15, 2000

Nearby stars of the Galactic disk and halo. II. ⋆

Klaus Fuhrmann

Institut für Astronomie und Astrophysik der Universität München, Scheinerstraße 1, 81679 München, Germany

Received date; accepted date

Abstract. Model atmosphere analyses of high resolution, high signal-to-noise échelle spectra are presented for a *second* set of fifty nearby F and G dwarfs. In combination with the precise Hipparcos astrometry, stellar evolutionary tracks, and the previous set of another fifty stars, it is shown that the chemical, kinematical, and age characteristics of the enlarged sample confirm the fairly reliable identification of *individual* halo, thick- and thin-disk stars, found earlier.

On account of this star-by-star classification, the data lend support for a thin disk that was most likely established about 9 Gyr ago and that is particularly discrete from the thick disk by a hiatus in star formation of no less than 3 Gyr. This, as well as the fact that the thick-disk's metallicity pre-enrichment ultimately solves the well-known G-dwarf problem, is taken as strong evidence for a thick-disk population as the *precursor* to the thin disk. By contrast, it is however not at all clear, whether a pre-existing halo population is actually required for the thick disk.

The kinematics of the identified thick-disk stars comes out with an asymmetric Strömberg drift of about -80 km s^{-1} with respect to the old thin disk, a value which is considerably lower than many contemporary estimates. In addition, we find a total space velocity of ~ 85 km s^{-1} as an appropriate *upper* limit to pre-select most of the stars of the thin disk.

For a subsample of the F and G dwarfs of the thin-disk population, which is by now volume-complete for one-third of these objects, the metallicity distribution functions for iron and the α-element magnesium peak at $\langle$ [Fe/H] $\rangle = -0.02$ and $\langle$ [Mg/H] $\rangle = +0.02$, that is, very close to the *solar* values. The corresponding age-metallicity relations for the thin disk result in Δ[Fe/H]$\sim$ 0.011 dex Gyr^{-1} and Δ[Mg/H]$\sim$ 0.006 dex Gyr^{-1}. This is an increase of 20% within 9 billion years for the iron content and a mere 12% for magnesium. In combination with the mean abundances of the thick-disk stars of our sample, $\langle$ [Fe/H] $\rangle = -0.59$ and $\langle$ [Mg/H] $\rangle = -0.21$, this implies the production of large amounts of iron for the intervening star-formation gap phase, and likewise a major contribution for both, Fe and Mg, at the onset of the thin disk.

Our data suggest that, not unexpected, only about 4% of the local F, G, and evolved K stars belong to the thick disk. But this number raises to $\sim$ 17% if we confine the star counts to long-lived objects, as is required for a fair study of Galactic evolution. Along with current estimates of the disk populations' vertical and radial scale-height ratios this implies for the *global* characteristics *either* a thick-disk mass contribution comparable to that of the thin disk, i.e. a considerable amount of baryonic dark matter for the Milky Way Galaxy, *or* a thick-disk initial mass function that has a cut-off at $\sim 0.7 M_{\odot}$ as is suggestive by the work of Favata, Micela & Sciortino (1997). The latter case then argues for a bimodal disk initial mass function as envisaged by Larson (1986), and, consequently, a large amount of baryonic thick-disk dark matter as well, this time however *remnant-dominated*.

Whichever scenario is the correct one remains yet to be settled, but with respect to all ever formed disk stars with masses above $\sim 0.7 M_{\odot}$ our data readily support a *rate* of star formation must have been extremely high within the earliest epoch of the Galaxy, some ∼12-14 Gyr ago. Thus it seems likely that part of the recent microlensing measurements, which favour a considerable fraction of the Galactic dark halo to consist of very old, i.e. dim, white dwarfs, may indeed be the relics of this ancient thick-disk population.

Key words: stars: fundamental parameters – stars: late-type – stars: white dwarfs – Galaxy: evolution – Galaxy: formation – dark matter

1. Introduction

The local history and geography, recorded in the spectra of unevolved stars, is one of the basic means for detailed studies in galactic astronomy. The solar neighborhood, defined here as the region within ∼100 pc, contains thousands of bright F- and G-type dwarfs, the distances of which are now known to better than 5% for a large percentage of them as a result of the very successful Hipparcos mission. This in turn has opened a number of closed doors: starting with precise stellar luminosities, an improved knowledge of surface gravities, effective temperatures, radii, masses, metallicities, kinematics, and stellar age-

⋆ Based on observations at the German Spanish Astronomical Center, Calar Alto, Spain datings is now at hand. Thus, a fairly complete *network* of the basic stellar parameters of unevolved F- and G-type stars (main sequence, turnoff and subgiants) has become possible from the combination of space-borne astrometry, stellar evolution and model atmosphere calculations, as well as high-resolution + high-signal-to-noise spectroscopy that ultimately provides the base for an *individual* classification of stars in terms of stellar populations, and thereby for a solid study of these fossil records in a Galactic context.

In a previous analysis of nearby F and G dwarfs of the Galactic disk and halo (Fuhrmann 1998, hereafter referred to as Paper I) we have already presented a number of details in this respect. Our work was however restricted to a rather small sample of only fifty stars. To improve the statistical significance of the previous study, we include here another fifty stars, most of which are actually within 25 pc, i.e. they are members of the Gliese & Jahreiß *Catalogue of Nearby Stars* (CNS4).

As we will show in the present analysis, the basic result of Paper I, namely the good separability of thick- and thin-disk stars – with all its consequences for the Galactic scenario – is still valid. Even more, the enlarged sample implies that the heretofore suggested age gap between both disk populations had a duration of no less than 3 Gyr. To put this in absolute numbers: thin-disk stars evidently do not exceed ~ 9 Gyr, whereas thick-disk stars are throughout very old objects, with a lower limit of ~ 12 Gyr. Thus on the base of these findings and the feasibility to pin down the population membership of individual stars we regard this as *an ultimate confirmation on the definite existence of the Gilmore & Reid's (1983) thick disk*[1].

It will also be seen that the fairly large break in the star forming evolution of both disk populations is also noticeably reflected in the stars' kinematics. We derive for the identified thick-disk stars a considerable mean asymmetric Strömberg drift of $\langle \Delta V_{rot} \rangle \sim -100$ km s^{-1} with respect to the local standard of rest. This is clearly at variance with a number of published studies that advocate values as low as -30 km s^{-1}, but ties in with the early work of Wyse & Gilmore (1986).

On the base of the individual identification of thick- and thin-disk stars, we will discuss the stars' chemistry, in particular two metallicity distribution functions (Mg, Fe) for the thin disk and their respective age-metallicity relations. We also present estimates on the local and global percentage of the dwarfs and giants observed in both disk populations. In the context of the formation and evolution of the Milky Way Galaxy this particularly raises the important question which of these stars are *short-lived* and which are *long-lived*. It thus touches upon the total fraction of thick-disk stars in the Galaxy including the stellar remnants (notably the white dwarfs), their putative contribution to baryonic dark matter, the thick-disk's initial mass function as well as star-formation rate.

[1] the reader may be interested to learn that I was not very convinced of the need for a thick-disk component in the Milky Way at the outset of this project. Since many follow-up kinematical studies had shown a considerably reduced rotational lag compared to the original papers on the thick disk, it was in fact one of my motivations to eventually disprove its existence

In the end one may realize that the inconspicuous appearance of the thick disk, which has by now lost all stars above $M \sim 0.95\ M_\odot$ to the realm of "darkness", is entirely superficial, and very reminiscent of the maxim: still waters run deep.

2. Observations

The spectra of our sample were obtained in the years 1996 through 2000 with the fiber-coupled Cassegrain échelle spectrograph FOCES (Pfeiffer et al. 1998) at the 2.2m telescope of the Calar Alto Observatory. Only few of them were exposed to a 1024^2 24μ CCD at $\lambda/\Delta\lambda \sim 35000$ and are limited to 4000-7000Å, whereas the standard configuration was a 2048^2 15μ CCD that covered 4000-9000Å at $\lambda/\Delta\lambda \sim 60000$. Again, all stars were observed at least twice, and with signal-to-noise values of at least S/N$\sim$150 up to S/N$\sim$400.

3. Applied methods

The basic stellar parameters are obtained in the same manner as described in Paper I. In brief, the work is *differential* with respect to the Sun. It is based on T. Gehren's (1975) LTE model atmosphere program, the Kitt Peak Solar Flux Atlas (Kurucz et al. 1984), and is a line profile analysis of the observed absorption line spectra. Below we give a short summary of the applied methods.

Effective temperature

the wings of the Balmer lines Hα and Hβ are used for the effective temperature determination. For metal-poor stars, Hγ and Hδ are also taken into account.

Surface gravity

this parameter is – in a first reduction step – derived from the LTE iron ionization equilibrium, which is hereafter labeled as case "I.E.". Comparison to the strong line wings of the Mg Ib triplet, however, requires a correction of $\log\ g$ to higher values for many of the hotter or evolved stars (case "S.L.").

Metallicities

iron abundances are based on Fe I and Fe II lines for I.E.-analyses, but refer to Fe II lines only, for the S.L.-analyses. Similarly [Fe/Mg] abundance ratios are either tabulated as [Fe/Mg I] (case I.E.), or [Fe I/Mg I] for S.L.-analyses.

Microturbulence

this parameter is obtained in the usual way in an iterative procedure along with $\log\ g$ and [Fe/H] (case I.E.). For S.L.-analyses, the tabulated microturbulence values result from Fe II lines only.

Macroturbulence & rotational velocity

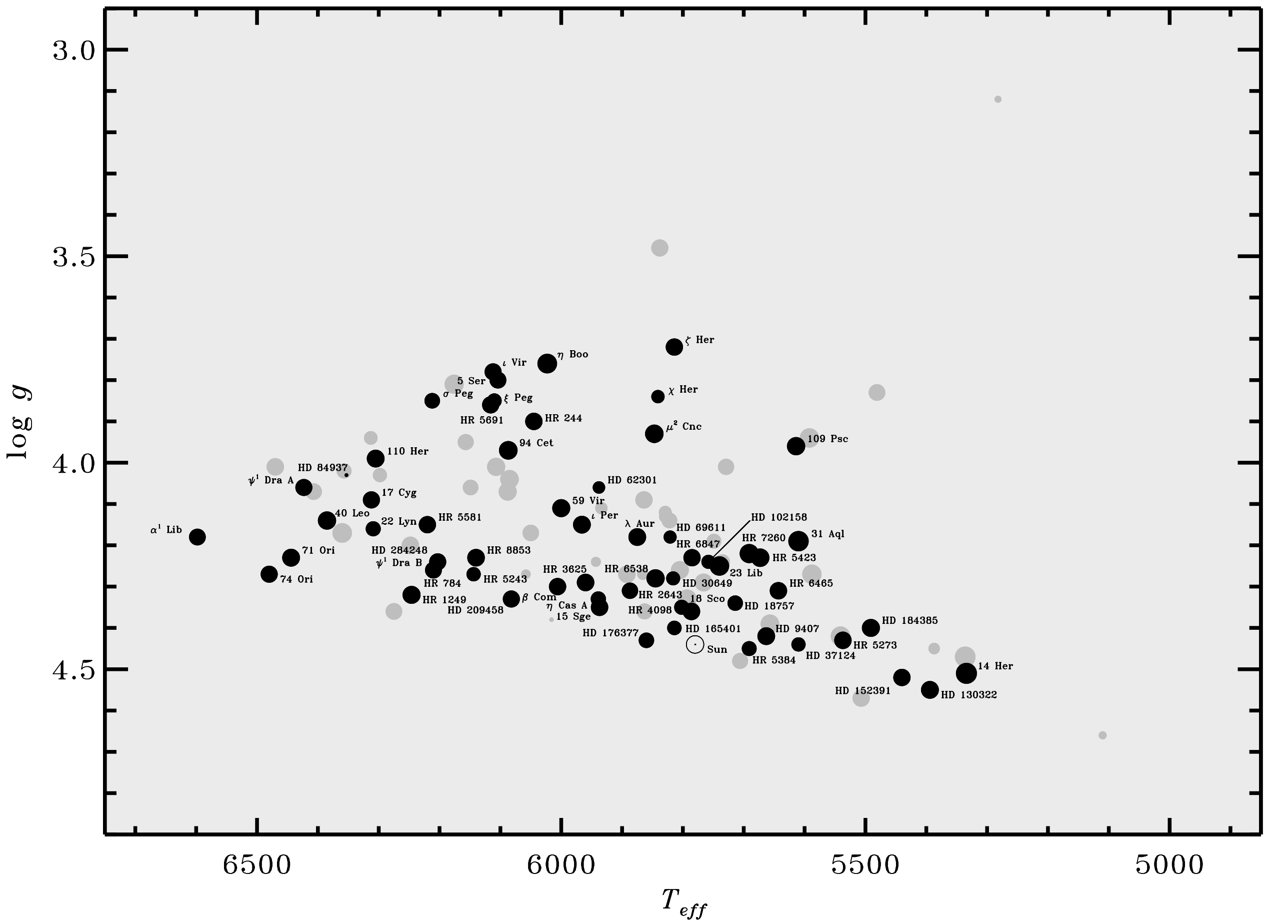

Fig. 1. The T_{eff}-log g *Kiel diagram* of the program stars. Circle diameters are in proportion to the metallicities. The grayscale symbols depict the stars of Paper I; the position of the Sun is indicated as well

we employ the macroturbulence parameter ζ in the radial-tangential form and adopt values as prescribed in Gray (1984, 1992), with some allowance to slightly smaller values ($\sim$0.5 km s^{-1}) for stronger lines (cf. Gray 1977).

Along with the known instrumental profile (obtained from Moon spectra) the projected rotational velocity is obtained as the residual to the observed line profiles. Note that our tabulated $v\sin i$'s must be understood *in combination* with the adopted ζ_{RT} values.

Visual apparent magnitude & reddening

is adopted from Mermilliod, Mermilliod & Hauck (1997). Reddening corrections are based on a star's Strömgren photometry and the formulae given in Schuster & Nissen (1989). We note however that in the sample of Table 1 it is only the halo star HD 84937 which is found to be slightly reddened by $A_V \simeq 0.11$ mag.

Absolute bolometric magnitude & bolometric correction

the absolute bolometric magnitude is calculated from the Hipparcos parallax, the (reddening corrected) V magnitude of a star, and the bolometric correction tabulated in Alonso, Arribas & Martínez-Roger (1995). Note that in the latter work $BC_{V,\odot} = -0.12$ mag is adopted. With an 0.05 dex higher value our spectroscopic distance scale (see below) would increase by 2.4%.

Radius

is immediately obtained from the effective temperature and bolometric magnitude of a star.

Mass & age

the mass and age of a star are partly obtained from isochrones and evolutionary tracks (VandenBerg et al. 2000) kindly made available by Don VandenBerg. A good deal of the stars (mostly the more metal-rich ones) were also recently calculated by Jan Bernkopf from the University Observatory Munich. In Table 1 we give the stellar masses that are employed in deriving the spectroscopic parallaxes. The more subtle stellar *age* deter-

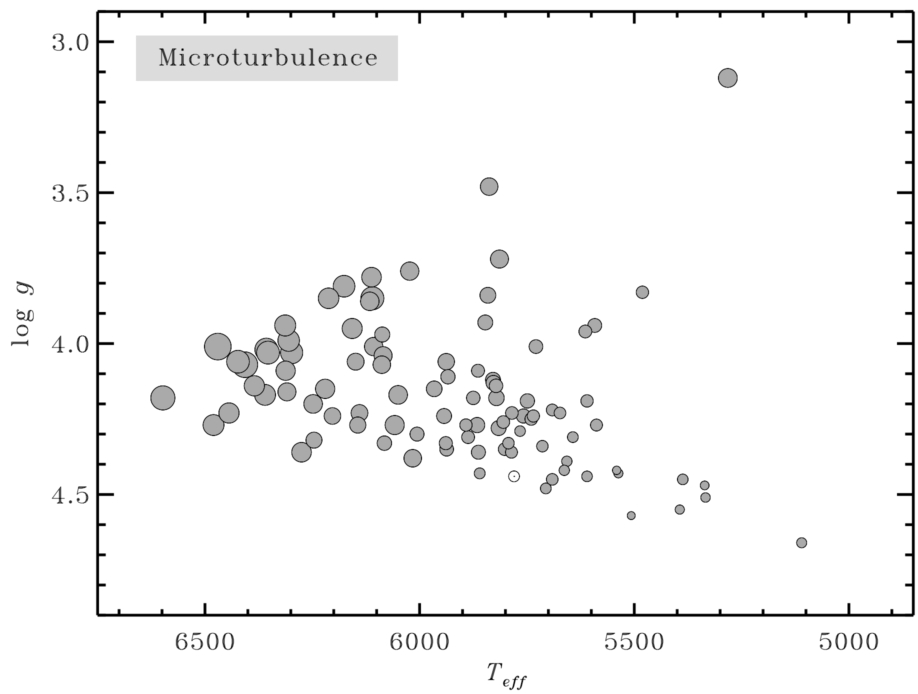

Fig. 2. The microturbulence dispersion. Circle diameters are in proportion to the ξ_t values. A smooth correlation along the main sequence and towards evolved stars is noticeable; the dependence on metallicity is weak

minations, on the other hand, are not yet explicitly tabulated, as part of them still lack a consistent treatment (cf. Bernkopf 1998). We defer this part to a forthcoming paper, as soon as the set of stellar masses and ages is homogeneous and complete.

Distance

spectroscopic parallaxes are calculated according to

$$\log \pi = 0.5([g] - [M]) - 2[T_{eff}] - 0.2(V + BC_V + 0.25)$$

with $M_{bol,\odot}$=4.75 and the usual logarithmic notation $[X]$ = log($X/X_\odot$). Agreement with the Hipparcos parallaxes to at least 85-90% is considered as a necessary, but by no means sufficient, condition for a trustworthy analysis.

Redundancy & zero point

for each star there are at least two spectra and hence at least two complete sets of stellar parameters. This redundancy is regarded as an indispensable test to assess the repeatability, which is typically given by 20 K, 0.03 dex, 0.02 dex, and 0.1 km s^{-1} for the effective temperature, surface gravity, metallicity, and microturbulence, respectively; the tabulated stellar parameters are a S/N-weighted average. All observing runs are complemented by Moon spectra and at least one or two standard stars. Thereby it is possible to intercompare the various runs and to test our zero point: the Sun *as a star*. In addition, systematic effects that might result from modified spectrograph settings, e.g. a change of CCDs, should also show up at this stage of analysis.

The most satisfactory result of these initial spectrograph tests is that the Moon spectra obtained at the latest campaigns provide the solar parameters to within the above given internal uncertainties. We interpret this as a consequence of the substantially higher resolution (R∼60000 vs 35000) and hence improved spectrum synthesis, and the better performance of the spectrograph fiber (i.e. a reduced noise level) that erases the systematic overabundances ($\sim 0.03 - 0.05$ dex) of the Moon spectra, which had plagued part of the observations before 1997.

Thus, both the confirmation of our zero point and the redundant information for all observed stars provide a firm base for the model atmosphere analyses, the results of which are now discussed.

4. Results

4.1. Basic stellar parameters

In Fig. 1 we show the complete sample of stars in the T_{eff}-$\log\ g$ *Kiel diagram*, those already presented in Paper I are indicated with grayscale symbols. Table 1 summarizes the stellar data in a similar manner as in Paper I. Each star is represented in two consecutive rows, one for the stellar parameters and the other for the corresponding error estimates. Most of the entries are self-explanatory; we mention that the uncertainties for the surface gravities, microturbulence velocities, Fe/Mg abundance ratios, and bolometric corrections are throughout adopted as 0.1 dex, 0.2 km s^{-1}, 0.05 dex, and 0.05 mag, respectively. The effective temperatures and metallicities have typical errors of $\Delta T_{eff} \sim 80$ K and Δ[Fe/H]~ 0.07 dex. As mentioned above, the macroturbulence values ζ_{RT} in column (10)

Table 1. Stellar parameters of the program stars. Most of the entries are self-explanatory; $\mathrm{d_{HIP}}$ in column (16) is the Hipparcos distance, $\mathrm{d_{sp}}$ in column (17) the spectroscopically deduced value, Δd the difference of both. For each star the second row indicates the error estimates. The macroturbulence value ζ_{RT} is generally *adopted* according to the relations given in Gray (1984, 1992), with only few small adjustments for metal-poor stars. The bolometric magnitudes in column (12) are based on the Hipparcos parallaxes, with bolometric corrections taken from Alonso, Arribas & Martínez-Roger (1995) and tabulated in column (13). Errors of $\log g$, ξ_t, [Fe/Mg] and BC_V are estimated to be 0.1 dex, 0.2 km s^{-1}, 0.05 dex and 0.05 mag, respectively. Uncertainties for the stellar masses are expected to be less than 10%. At the end of the table the outliers of Fig. 8 (see below) are listed separately

(1) Object	(2) HR	(3) HD	(4) V [mag]	(5) T_{eff} [K]	(6) $\log g$ [cgs]	(7) [Fe/H] [dex]	(8) ξ_t [km/s]	(9) [Fe/Mg] [dex]	(10) ζ_{RT} [km/s]	(11) $v\sin i$ [km/s]	(12) M_{bol} [mag]	(13) BC_V [mag]	(14) Mass [$M_\odot$]	(15) Radius [$R_\odot$]	(16) $\mathrm{d_{HIP}}$ [pc]	(17) $\mathrm{d_{sp}}$ [pc]	(18) Δd [%]
η Cas A	219	4614	3.444	5939	4.33	–0.30	1.06	–0.09	4.2	1.5	4.44	–0.13	0.96	1.09	5.95	6.07	1.9
			0.009	70	0.10	0.06	0.20	0.05		1.0	0.05	0.05		0.04	0.02	0.83	
		9407	6.530	5663	4.42	+0.03	0.87	–0.01	3.1	2.0	4.77	–0.15	0.97	1.03	20.99	20.49	–2.4
			0.000	70	0.10	0.06	0.20	0.05		1.0	0.06	0.05		0.04	0.27	2.80	
109 Psc	508	10697	6.260	5614	3.96	+0.10	1.04	+0.00	4.1	1.0	3.54	–0.15	1.13	1.84	32.56	32.53	–0.1
			0.000	80	0.10	0.06	0.20	0.05		1.0	0.08	0.05		0.09	0.88	4.47	
		18757	6.634	5714	4.34	–0.28	0.95	–0.32	3.3	1.0	4.68	–0.16	0.90	1.05	22.86	23.06	0.9
			0.030	70	0.10	0.07	0.20	0.05		1.0	0.07	0.05		0.04	0.45	3.17	
ι Per	937	19373	4.046	5966	4.15	+0.03	1.23	–0.01	4.8	2.4	3.83	–0.10	1.11	1.43	10.53	10.80	2.6
			0.008	70	0.10	0.06	0.20	0.05		1.0	0.05	0.05		0.05	0.07	1.47	
94 Cet	962	19994	5.068	6087	3.97	+0.14	1.19	+0.01	5.2	8.4	3.24	–0.08	1.31	1.80	22.38	24.30	8.6
			0.021	80	0.10	0.08	0.20	0.05		0.9	0.07	0.05		0.07	0.38	3.34	
	1249	25457	5.380	6246	4.32	+0.06	1.25	+0.01	5.5	17.0	3.88	–0.08	1.22	1.27	19.23	19.12	–0.6
			0.012	80	0.10	0.09	0.20	0.05		1.0	0.06	0.05		0.05	0.28	2.62	
		30649	6.973	5816	4.28	–0.47	1.18	–0.35	3.9	1.0	4.44	–0.15	0.88	1.13	29.90	29.64	–0.9
			0.016	70	0.10	0.07	0.20	0.05		1.0	0.09	0.05		0.06	1.04	4.05	
λ Aur	1729	34411	4.708	5875	4.18	+0.03	1.08	–0.04	4.0	1.0	4.08	–0.12	1.05	1.31	12.65	13.28	5.0
			0.013	70	0.10	0.06	0.20	0.05		1.0	0.06	0.05		0.05	0.15	1.81	
		37124	7.664	5610	4.44	–0.44	0.89	–0.32	3.0	1.0	4.88	–0.18	0.84	1.00	33.24	30.41	–8.5
			0.015	70	0.10	0.08	0.20	0.05		1.0	0.10	0.05		0.05	1.32	4.16	
71 Ori	2220	43042	5.195	6444	4.23	+0.04	1.52	+0.00	6.2	3.5	3.51	–0.06	1.29	1.42	21.13	21.44	1.5
			0.008	80	0.10	0.06	0.20	0.05		0.7	0.06	0.05		0.06	0.39	2.93	
74 Ori	2241	43386	5.039	6480	4.27	–0.06	1.56	–0.06	6.4	19.4	3.51	–0.07	1.27	1.40	19.61	19.07	–2.8
			0.006	80	0.10	0.07	0.20	0.05		0.9	0.06	0.05		0.05	0.35	2.61	
	2643	52711	5.928	5887	4.31	–0.16	1.04	–0.04	4.2	2.0	4.40	–0.13	0.99	1.13	19.09	19.46	1.9
			0.007	70	0.10	0.05	0.20	0.05		1.0	0.06	0.05		0.04	0.31	2.66	
22 Lyn	2849	58855	5.368	6309	4.16	–0.32	1.38	–0.12	5.9	8.0	3.78	–0.10	1.09	1.31	19.90	21.83	9.7
			0.013	80	0.10	0.06	0.20	0.05		0.8	0.06	0.05		0.05	0.33	2.99	
		62301	6.749	5938	4.06	–0.69	1.28	–0.30	4.2	1.0	3.93	–0.15	0.86	1.38	34.22	35.52	3.8
			0.023	80	0.10	0.07	0.20	0.05		1.0	0.09	0.05		0.07	1.16	4.88	
μ^2 Cnc	3176	67228	5.296	5847	3.93	+0.12	1.18	+0.00	4.7	3.1	3.34	–0.11	1.21	1.86	23.33	24.70	5.9
			0.008	70	0.10	0.06	0.20	0.05		0.8	0.07	0.05		0.08	0.54	3.37	
		69611	7.717	5821	4.18	–0.60	1.22	–0.43	4.1	1.0	4.11	–0.16	0.85	1.32	48.88	46.00	–5.9
			0.022	80	0.10	0.07	0.20	0.05		1.0	0.14	0.05		0.09	2.94	6.33	
		84937	8.319	6353	4.03	–2.07	1.68	–0.36	5.4	1.0	3.50	–0.18	0.80	1.46	80.39	78.33	–2.6
			0.023	80	0.10	0.09	0.20	0.05		1.0	0.20	0.05		0.15	7.49	10.75	
40 Leo	4054	89449	4.793	6385	4.14	+0.09	1.52	–0.06	6.2	16.7	3.10	–0.06	1.40	1.74	21.17	20.22	–4.5
			0.008	80	0.10	0.07	0.20	0.05		1.0	0.06	0.05		0.07	0.37	2.77	
	4098	90508	6.445	5802	4.35	–0.33	1.02	–0.22	3.4	1.0	4.44	–0.15	0.94	1.14	23.56	22.12	–6.1
			0.014	70	0.10	0.07	0.20	0.05		1.0	0.07	0.05		0.04	0.44	3.02	
		102158	8.056	5758	4.24	–0.46	1.13	–0.40	3.7	1.0	4.31	–0.16	0.85	1.23	52.16	49.11	–5.9
			0.015	80	0.10	0.08	0.20	0.05		1.0	0.11	0.05		0.07	2.48	6.75	
β Com	4983	114710	4.256	6006	4.30	–0.03	1.12	–0.01	4.5	3.9	4.34	–0.10	1.06	1.11	9.15	9.92	8.3
			0.012	70	0.10	0.07	0.20	0.05		1.0	0.05	0.05		0.04	0.06	1.35	
η Boo	5235	121370	2.680	6023	3.76	+0.28	1.40	–0.03	5.6	12.8	2.33	–0.08	1.62	2.80	11.34	11.23	–1.0
			0.009	70	0.10	0.07	0.20	0.05		0.8	0.05	0.05		0.10	0.10	1.53	
	5243	121560	6.170	6144	4.27	–0.43	1.26	–0.15	5.2	1.0	4.13	–0.12	1.02	1.17	24.22	25.28	4.4
			0.010	80	0.10	0.07	0.20	0.05		1.0	0.07	0.05		0.05	0.47	3.46	
	5273	122742	6.302	5537	4.43	–0.01	0.78	–0.03	2.6	1.8	5.03	–0.18	0.92	0.96	16.60	16.78	1.1
			0.036	80	0.10	0.07	0.20	0.05		1.0	0.07	0.05		0.04	0.22	2.32	

(1) Object	(2) HR	(3) HD	(4) V [mag]	(5) T_{eff} [K]	(6) $\log g$ [cgs]	(7) [Fe/H] [dex]	(8) ξ_t [km/s]	(9) [Fe/Mg] [dex]	(10) ζ_{RT} [km/s]	(11) $v\sin i$ [km/s]	(12) M_{bol} [mag]	(13) BC_V [mag]	(14) Mass [$M_\odot$]	(15) Radius [$R_\odot$]	(16) $\mathrm{d_{HIP}}$ [pc]	(17) $\mathrm{d_{sp}}$ [pc]	(18) Δd [%]
ι Vir	5338	124850	4.077	6112	3.78	–0.06	1.48	–0.04	5.9	15.3	2.33	–0.09	1.46	2.71	21.39	20.30	–5.1
			0.010	70	0.10	0.09	0.20	0.05		1.0	0.07	0.05		0.10	0.41	2.77	
	5384	126053	6.269	5691	4.45	–0.35	0.96	–0.14	3.2	1.5	4.88	–0.16	0.89	0.97	17.60	16.88	–4.1
			0.010	70	0.10	0.07	0.20	0.05		1.0	0.06	0.05		0.04	0.33	2.31	
	5423	127334	6.354	5691	4.22	+0.21	0.97	–0.01	3.5	1.0	4.36	–0.14	1.07	1.23	23.57	25.39	7.7
			0.005	70	0.10	0.07	0.20	0.05		1.0	0.06	0.05		0.05	0.33	3.47	
		130322	8.036	5394	4.55	+0.04	0.79	+0.02	2.1	1.5	5.46	–0.21	0.93	0.83	29.76	30.49	2.5
			–	80	0.10	0.06	0.20	0.05		1.0	0.11	0.05		0.05	1.40	4.20	
α^1 Lib	5530	130819	5.150	6598	4.18	–0.10	1.76	–0.04	6.9	3.0	3.21	–0.06	1.33	1.55	23.66	23.66	0.0
			0.011	80	0.10	0.07	0.20	0.05		1.0	0.07	0.05		0.07	0.60	3.23	
	5581	132254	5.639	6220	4.15	–0.03	1.46	–0.03	5.5	7.5	3.58	–0.08	1.18	1.47	24.84	25.47	2.5
			0.010	80	0.10	0.07	0.20	0.05		0.8	0.06	0.05		0.06	0.34	3.49	
23 Lib	5657	134987	6.443	5740	4.25	+0.25	1.02	+0.00	3.5	1.5	4.27	–0.13	1.12	1.26	25.65	26.73	4.2
			0.004	70	0.10	0.07	0.20	0.05		1.0	0.07	0.05		0.05	0.66	3.65	
	5691	136064	5.137	6116	3.86	–0.05	1.41	–0.05	5.8	3.8	3.03	–0.09	1.20	1.96	25.31	27.39	8.2
			0.018	80	0.10	0.07	0.20	0.05		0.9	0.06	0.05		0.08	0.30	3.76	
χ Her	5914	142373	4.622	5841	3.84	–0.57	1.24	–0.22	4.4	1.0	3.47	–0.15	0.97	1.76	15.85	17.63	11.2
			0.015	70	0.10	0.07	0.20	0.05		1.0	0.06	0.05		0.06	0.14	2.41	
14 Her		145675	6.655	5334	4.51	+0.45	0.81	+0.00	1.9	2.0	5.14	–0.22	1.11	0.98	18.15	17.98	–0.9
			0.008	90	0.10	0.07	0.20	0.05		1.0	0.06	0.05		0.04	0.20	2.49	
18 Sco	6060	146233	5.504	5786	4.36	+0.01	0.98	–0.03	3.6	1.5	4.64	–0.13	0.99	1.05	14.03	14.57	3.9
			0.015	60	0.10	0.06	0.20	0.05		1.0	0.06	0.05		0.04	0.18	1.98	
ζ Her[1)]	6212	150680	2.900	5814	3.72	–0.03	1.38	–0.05	4.9	3.9	2.61	–0.13	1.37	2.64	10.80	10.92	1.1
			–	70	0.10	0.07	0.20	0.05		1.0	0.05	0.05		0.09	0.07	1.49	
	6465	157347	6.283	5643	4.31	–0.01	0.90	–0.02	3.2	2.0	4.68	–0.16	0.93	1.08	19.46	20.14	3.5
			0.004	70	0.10	0.06	0.20	0.05		1.0	0.06	0.05		0.04	0.33	2.75	
ψ^1 Dra A	6636	162003	4.590	6423	4.06	–0.07	1.67	–0.04	6.7	11.1	2.80	–0.07	1.44	1.97	22.04	20.64	–6.3
			0.014	80	0.10	0.07	0.20	0.05		0.8	0.07	0.05		0.08	0.41	2.83	
ψ^1 Dra B	6637	162004	5.810	6203	4.24	–0.06	1.29	–0.03	5.3	5.4	3.98	–0.09	1.15	1.23	22.32	24.34	9.0
			0.014	70	0.10	0.06	0.20	0.05		0.8	0.11	0.05		0.07	1.01	3.32	
	6847	168009	6.295	5785	4.23	–0.03	1.03	–0.04	3.8	1.5	4.38	–0.13	0.97	1.18	22.69	24.09	6.2
			0.006	70	0.10	0.06	0.20	0.05		1.0	0.06	0.05		0.04	0.27	3.29	
110 Her	7061	173667	4.201	6305	3.99	+0.03	1.60	–0.04	6.2	18.0	2.73	–0.07	1.47	2.12	19.09	18.21	–4.6
			0.010	80	0.10	0.10	0.20	0.05		1.0	0.06	0.05		0.08	0.25	2.49	
		176377	6.790	5860	4.43	–0.27	0.91	–0.07	3.9	2.0	4.80	–0.14	0.97	0.94	23.43	24.61	5.0
			–	70	0.10	0.07	0.20	0.05		1.0	0.06	0.05		0.03	0.36	3.36	
	7260	178428	6.074	5673	4.23	+0.12	0.96	–0.04	3.6	1.5	4.32	–0.14	1.03	1.26	20.96	21.44	2.3
			0.012	70	0.10	0.06	0.20	0.05		1.0	0.06	0.05		0.05	0.34	2.93	
31 Aql	7373	182572	5.155	5610	4.19	+0.37	1.01	+0.00	3.5	2.0	4.11	–0.15	1.18	1.42	15.15	15.36	1.4
			0.016	80	0.10	0.07	0.20	0.05		1.0	0.06	0.05		0.06	0.18	2.11	
17 Cyg	7534	187013	4.989	6312	4.09	–0.05	1.46	–0.08	6.1	9.1	3.32	–0.08	1.24	1.62	20.86	21.42	2.7
			0.018	80	0.10	0.08	0.20	0.05		0.8	0.06	0.05		0.06	0.24	2.94	
15 Sge	7672	190406	5.795	5937	4.35	–0.01	1.10	+0.01	4.2	2.0	4.45	–0.11	1.06	1.08	17.67	18.52	4.8
			0.008	70	0.10	0.07	0.20	0.05		1.0	0.06	0.05		0.04	0.24	2.53	
		209458	7.655	6082	4.33	–0.06	1.15	–0.03	4.7	3.0	4.19	–0.10	1.08	1.16	47.08	47.56	1.0
			0.008	70	0.10	0.06	0.20	0.05		0.8	0.12	0.05		0.07	2.33	6.49	
ξ Peg	8665	215648	4.197	6110	3.85	–0.37	1.69	–0.18	5.8	7.9	3.03	–0.11	1.12	1.97	16.25	17.16	5.6
			0.008	80	0.10	0.07	0.20	0.05		0.8	0.06	0.05		0.07	0.21	2.35	
σ Peg	8697	216385	5.162	6212	3.85	–0.26	1.54	–0.11	5.8	1.0	2.92	–0.10	1.17	2.00	26.85	28.48	6.1
			0.018	80	0.10	0.07	0.20	0.05		1.0	0.07	0.05		0.08	0.56	3.91	
	8853	219623	5.577	6140	4.23	+0.01	1.30	–0.01	5.3	3.6	3.95	–0.09	1.14	1.27	20.28	21.57	6.3
			0.015	80	0.10	0.07	0.20	0.05		1.0	0.06	0.05		0.05	0.24	2.96	
	244	5015	4.797	6045	3.90	–0.02	1.39	–0.08	5.6	5.3	3.36	–0.10	1.17	1.73	18.57	21.53	15.9
			0.012	80	0.10	0.07	0.20	0.05		0.8	0.06	0.05		0.07	0.21	2.95	
5 Ser	5694	136202	5.055	6104	3.80	–0.09	1.45	–0.04	5.6	2.0	2.99	–0.10	1.23	2.00	24.72	28.45	15.1
			0.007	80	0.10	0.07	0.20	0.05		1.0	0.07	0.05		0.08	0.50	3.90	
	6538	159222	6.541	5845	4.28	+0.09	1.05	+0.00	4.1	1.5	4.55	–0.12	1.08	1.07	23.70	27.61	16.5
			0.025	70	0.10	0.07	0.20	0.05		1.0	0.06	0.05		0.04	0.32	3.78	
G 8-16		284248	9.234	6202	4.23	–1.61	1.55	–0.38	3.2	1.0	4.60	–0.18	0.76	0.93	77.88	92.83	19.2
			0.017	80	0.10	0.07	0.20	0.05		1.0	0.24	0.05		0.11	9.00	12.73	

[1)] the V magnitude of the primary is taken from the *Bright Star Catalogue*

Table 2. Revised stellar analyses for stars of Paper I

(1) Object	(2) HR	(3) HD	(4) V [mag]	(5) T_{eff} [K]	(6) $\log g$ [cgs]	(7) [Fe/H] [dex]	(8) ξ_t [km/s]	(9) [Fe/Mg] [dex]	(10) ζ_{RT} [km/s]	(11) $v\sin i$ [km/s]	(12) M_{bol} [mag]	(13) BC_V [mag]	(14) Mass [$M_\odot$]	(15) Radius [$R_\odot$]	(16) d_{HIP} [pc]	(17) d_{sp} [pc]	(18) Δd [%]
		22879	6.689	5866	4.27	–0.86	1.20	–0.44	4.1	1.0	4.59	–0.17	0.80	1.04	24.35	25.33	4.0
			0.009	80	0.10	0.07	0.20	0.05		1.0	0.07	0.05		0.04	0.52	3.48	
70 Vir	5072	117176	4.975	5481	3.83	–0.11	1.01	–0.08	3.9	1.0	3.50	–0.19	1.07	1.97	18.11	19.10	5.5
			0.008	70	0.10	0.07	0.20	0.05		1.0	0.06	0.05		0.07	0.24	2.61	
ϵ Lib	5723	137052	4.929	6298	3.92	+0.00	1.68	–0.02	6.5	10.2	2.31	–0.07	1.56	2.58	32.36	28.34	–12.4
			0.005	80	0.10	0.08	0.20	0.05		0.8	0.09	0.05		0.12	1.07	3.88	
ρ CrB	5968	143761	5.412	5822	4.14	–0.24	1.09	–0.20	4.1	1.0	4.07	–0.14	0.97	1.34	17.43	17.97	3.1
			0.016	70	0.10	0.08	0.20	0.05		1.0	0.06	0.05		0.05	0.22	2.46	
μ Her	6623	161797	3.417	5592	3.94	+0.24	1.11	+0.00	4.0	1.0	3.64	–0.15	1.14	1.77	8.40	8.96	6.7
			0.014	70	0.10	0.07	0.20	0.05		1.0	0.05	0.05		0.06	0.04	1.23	
	7569	187923	6.142	5729	4.01	–0.17	1.10	–0.21	4.1	1.0	3.79	–0.15	1.01	1.58	27.66	28.76	4.0
			0.015	70	0.10	0.08	0.20	0.05		1.0	0.07	0.05		0.07	0.62	3.93	

Table 3. Rejected stellar analyses: the tabulated stars are all chromospherically active and come out with modeling discordances for the Mg Ib line profiles. Except for HR 784 and HD 165401, the data refer to the results from the LTE iron ionization equilibrium method

(1) Object	(2) HR	(3) HD	(4) V [mag]	(5) T_{eff} [K]	(6) $\log g$ [cgs]	(7) [Fe/H] [dex]	(8) ξ_t [km/s]	(9) [Fe/Mg] [dex]	(10) ζ_{RT} [km/s]	(11) $v\sin i$ [km/s]	(12) M_{bol} [mag]	(13) BC_V [mag]	(14) Mass [$M_\odot$]	(15) Radius [$R_\odot$]	(16) d_{HIP} [pc]	(17) d_{sp} [pc]	(18) Δd [%]
	784	16673	5.775	6210	4.26	–0.09	1.26	–0.03	5.3	6.2	4.02	–0.09	1.13	1.21	21.54	23.24	7.9
			0.005	80	0.10	0.07	0.20	0.05		0.9	0.06	0.05		0.05	0.39	3.18	
	3625	78366	5.964	5960	4.29	+0.00	1.10	+0.01	4.3	3.5	4.45	–0.11	1.07	1.08	19.14	21.76	13.7
			0.030	80	0.10	0.07	0.20	0.05		0.9	0.07	0.05		0.05	0.32	3.00	
59 Vir	5011	115383	5.211	6000	4.11	+0.06	1.25	–0.02	5.0	6.6	3.84	–0.10	1.13	1.40	17.95	19.80	10.3
			0.011	70	0.10	0.07	0.20	0.05		0.8	0.06	0.05		0.05	0.28	2.70	
		152391	6.640	5440	4.52	–0.03	0.92	+0.03	2.3	3.3	5.30	–0.20	0.89	0.87	16.94	16.60	–2.0
			0.010	80	0.10	0.08	0.20	0.05		1.0	0.06	0.05		0.04	0.25	2.29	
		165401	6.804	5814	4.40	–0.41	1.09	–0.34	3.7	1.5	4.72	–0.15	0.93	1.00	24.39	24.57	0.7
			0.008	80	0.10	0.07	0.20	0.05		1.0	0.07	0.05		0.04	0.53	3.37	
		184385	6.889	5491	4.40	+0.06	0.92	+0.02	2.4	2.5	5.18	–0.18	0.95	0.90	20.16	22.67	12.5
			0.006	80	0.10	0.07	0.20	0.05		1.0	0.07	0.05		0.04	0.39	3.12	

are generally taken from Gray (1984, 1992), with only minor corrections for few metal-poor stars (with a tendency to lower values). Some of the stellar masses in column (14) are presumably subject to small systematic corrections, typically less than 5%. The general uncertainties of the stellar masses are assessed to be less than 10%. At the end of Table 1 the small separate group presents those objects that show inconsistencies with the Hipparcos parallaxes, as detailed in columns (16) – (18) and Fig. 8 below.

At the most recent observing runs, some of our objects were re-investigated, partly because they had earlier been found to be discrepant or interesting cases, or simply because they were used for calibration purposes (e.g. 70 Vir, HD 22879). The resulting updates of the stellar parameters are given in Table 2 and replace those of Paper I. The re-analysis of the spectroscopic binary ϵ Lib, however, shows that it remains a discrepant case (cf. Fig. 8).

In Table 3 we tabulate chromospherically active stars, the derived stellar parameters of which we ultimately rejected (see

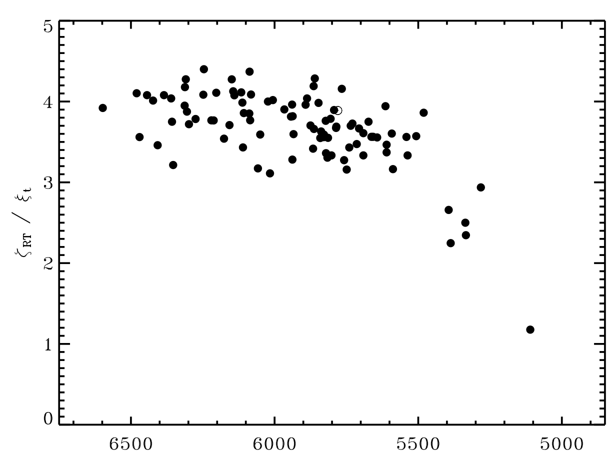

Fig. 3. Correlation of the macro-/microturbulence ratio vs effective temperature. The position of the Sun is indicated as well

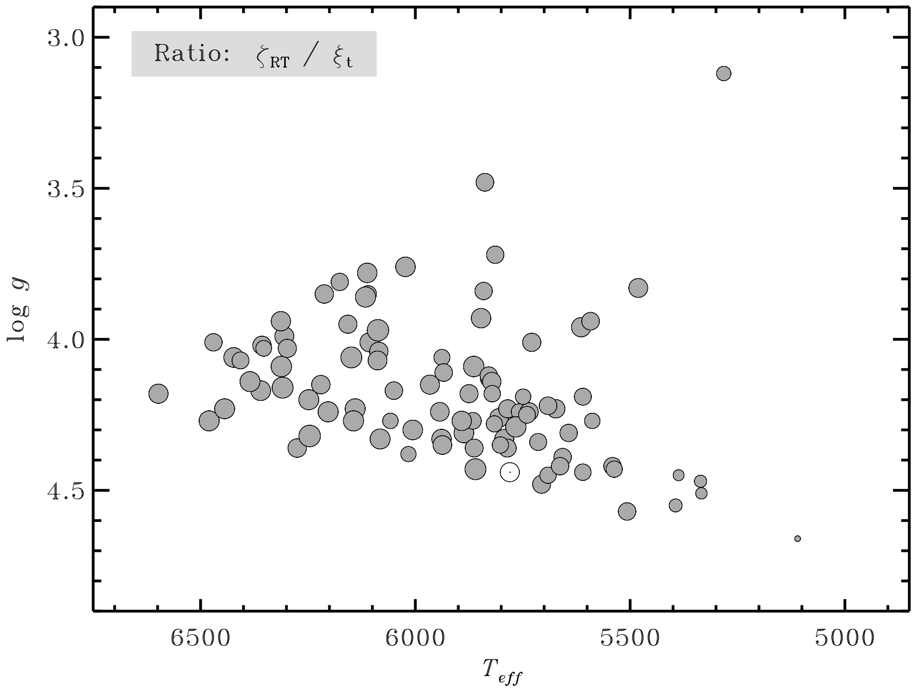

Fig. 4. Same as Fig. 3, but displayed in the T_{eff}-log g plane

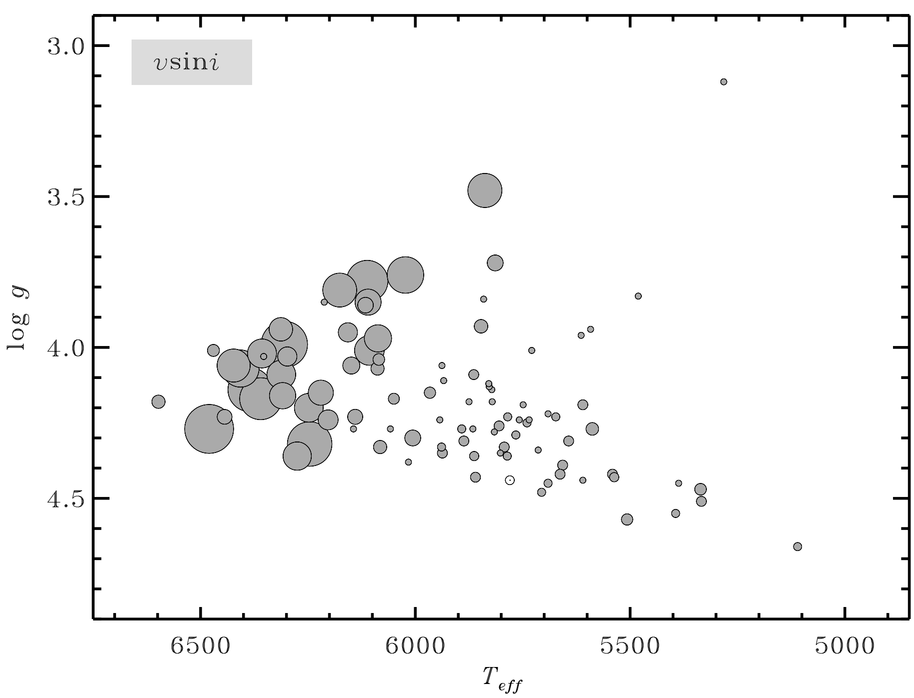

Fig. 5. Distribution of the projected rotational velocities. The diagram confirms the well-known finding of a marked onset to high $v\sin i$ values for F-type stars. The largest circle corresponds to $v\sin i = 19$ km s^{-1}

Sect. 4.2, in particular HD 152391). Note that HD 165401 is a re-analyzed star of Paper I.

With a sample that contains approximately twice as many stars compared to our previous analysis we now ask: what is the distribution of these objects with respect to micro- and macroturbulence, projected rotational velocity, stellar radius and mass? The answer is given in Figs. 2 to 7, which indicate that most of the characteristics remain actually unchanged and consequently need not be re-discussed here. It is only one feature of Fig. 5, the distribution of $v\sin i$ velocities, that we must comment on. While we have argued in Paper I that slow rotators are generally found below $T_{eff} \sim 6100$ K, with 44 And being the only discrepant case, we now learn from Fig. 5 that the dividing line between fast and slow rotators is *tilted* in the T_{eff}-$\log g$ plane, which renders the position of 44 And no longer exceptional.

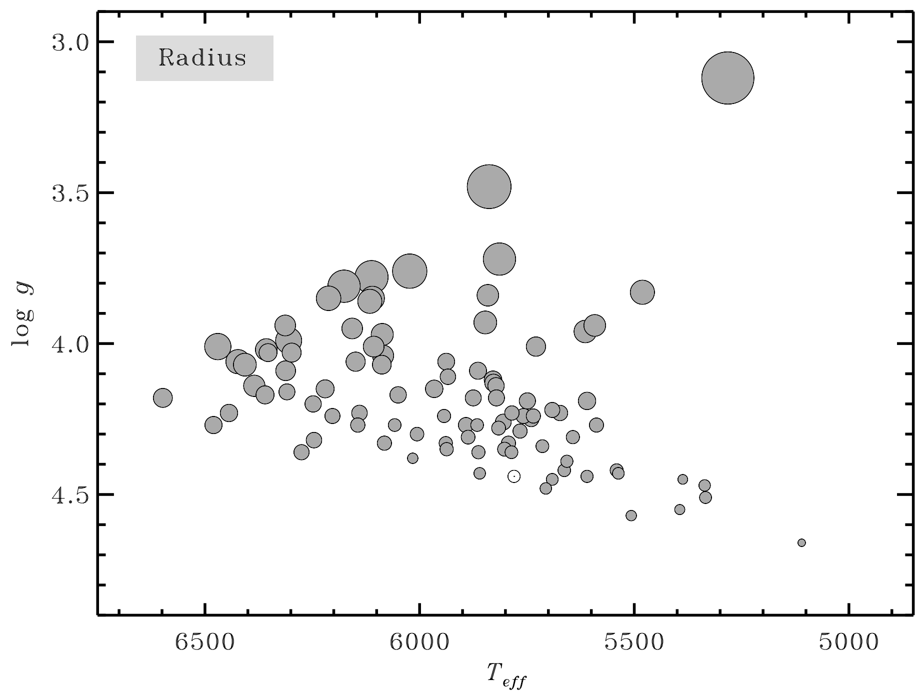

Fig. 6. Distribution of the stellar radii

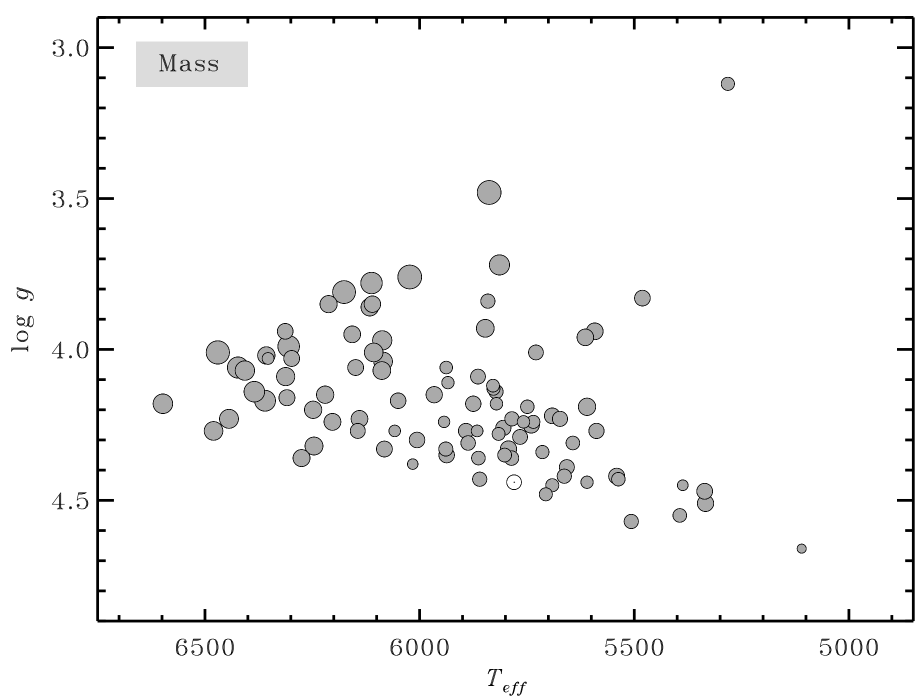

Fig. 7. Distribution of the stellar masses

The comparison of the spectroscopic and astrometric distance scales in Fig. 8 is also very similar to the results of the corresponding diagram of Paper I. We recall that the good correlation along the 1:1 line in Fig. 8 is basically a confirmation of the spectroscopically derived surface gravities: the mean 2.1% distance offset corresponds to less than $\Delta \log g$ ~0.02 dex (or $\Delta \log g$ ~0.04 dex, if we adopt $BC_{V,\odot} = -0.07$ mag, as discussed above). This in turn provides much confidence in the stellar metallicities, and, at least for those stars where the $\log g$ is based on the LTE iron ionization equilibrium (defined above as case I.E.) the effective temperature scale is also very trustworthy[2]. Thus Fig. 8 plays a key role in assessing the *reliability*

[2] we reiterate from Paper I that ΔT_{eff} ~20 K corresponds to $\Delta \log g$ ~0.04 dex, i.e. there is a close coupling of T_{eff} and $\log g$ in our model atmosphere analyses for stars below $T_{eff} \sim 6000$ K

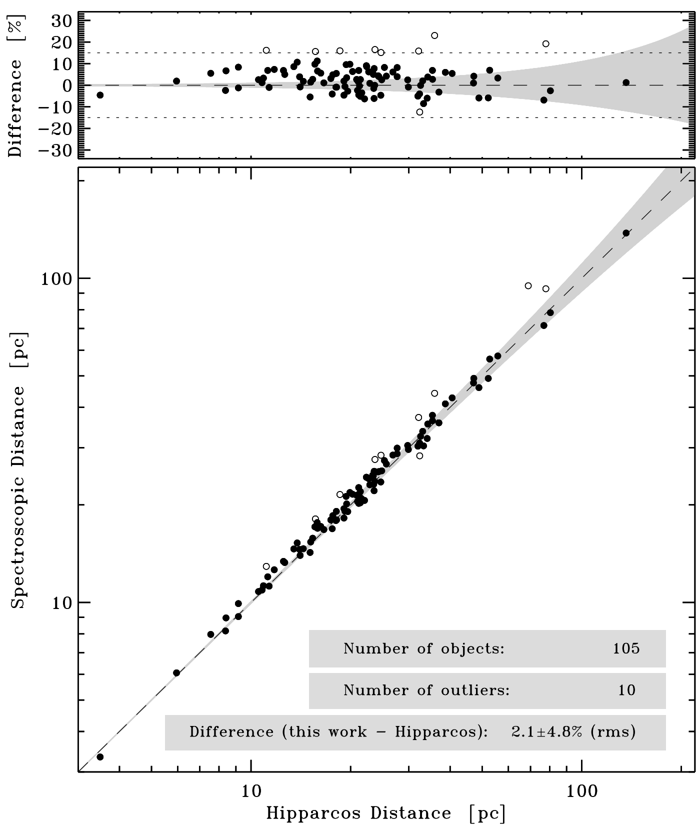

Suspected binaries
or variable stars:

G 78−1	at	68 pc	with	7.42 σ
79 Cet	at	35 pc	with	4.38 σ
G 8−16	at	77 pc	with	3.58 σ
ϵ Lib	at	32 pc	with	3.03 σ
HR 6538	at	23 pc	with	3.02 σ
γ Ser	at	11 pc	with	2.94 σ
HR 244	at	18 pc	with	2.90 σ
35 Dra	at	32 pc	with	2.87 σ
99 Her	at	15 pc	with	2.83 σ
5 Ser	at	24 pc	with	2.73 σ

Fig. 8. Comparison of the spectroscopic versus astrometric distance scale. Errors in the Hipparcos data are negligible below 10 pc, comparable around 100 pc and get worse beyond; the shaded wedge illustrates this behaviour for a typical parallax error of 1 mas. Statistical corrections to account for the possible bias in the astrometric data of the few more distant objects are very small and therefore neglected. Individual uncertainties of the spectroscopic data are about 10-15% (dotted curve), with no dependence on distance. The spectroscopic distances result in *higher* values by 2.1% on average, and a statistical *rms* error of 4.8%. The corresponding offset in the surface gravity parameter – to which this result is most susceptible – is less than $\Delta \log g$ ~0.02 dex. Consequently, the accuracy of the well-defined correlation reveals several outliers (open circles), most of which are supposed to be spectroscopic binaries

of the derived stellar parameters, in particular, since it also allows to exclude discrepant objects (e.g. spectroscopic binaries) from further consideration, as we have already done in Paper I. Note that almost all outliers in Fig. 8 come out to the left of the diagonal, that is, with *enlarged* spectroscopic distances. As such it is probable that part of the small distance offset is due to suspicious cases like 94 Cet (cf. Duquennoy & Mayor 1991), χ Her (see below), or ι Psc (see Eggen 1998a, p. 2414).

It must however also be realized, that, in principle, the coincidence of the spectroscopic and astrometric distance is a necessary, but not a sufficient, condition for a reliable stellar analysis. We present few such counter-examples in the next subsection.

4.2. Notes on individual stars

In this subsection we comment on some spectroscopic binaries or suspected candidates, as well as few other stars of particular interest.

HR 244: our data provide a suspicious Δd=15.9% (2.90σ) discrepancy with the Hipparcos distance scale. This may be explainable with the SB1 status suggested by Abt & Levy (1976). The latter finding is however not supported by the work of Morbey & Griffin (1987) and Duquennoy & Mayor (1991).

HR 784: the spectrum reveals chromospheric activities which may be induced from a nearby companion. Anderson & Kraft (1972) report a certain variable radial velocity for this star.

HR 1249: this is also a known EUV source (e.g. Pounds et al. 1993, Burleigh, Barstow & Fleming 1997); Duquennoy & Mayor (1991) note that the radial velocity may also be variable. Our spectra of the line cores of Hα and the Ca II infrared triplet suggest an enhanced level of chromospheric activity. The fairly high rotational velocity ($v\sin i = 17$ km s^{-1}) as well as high effective temperature ($T_{eff} = 6246$ K) however prohibit the study of details such as discussed in Fig.11 for the Mg Ib lines of HD 152391.

HR 3625: the star is known as a chromospherically active dwarf (cf. Smith & Churchill 1998) and reveals similar spectroscopic features as HD 152391, which we discuss below.

HR 4098: Eggen (1971) classified this star as a member of his “Arcturus Group” (but see also Eggen 1998a, p. 2413). As such (see below) one should expect a thick-disk membership. This conjecture is however only confirmed by the star’s kinematics. Neither its chemistry nor age lend further support to this finding (although we point out that the age estimate suffers from the rather unevolved stage, $\log g = 4.35$). Thus, HR 4098 seems to be best characterized as a disk "transition star" (see below).

β Com: the spectra show weak chromospheric signatures in the cores of Hα and the Ca II infrared triplet. This appears to be corroborated by inspection of the time series plots in Radick et al. (1998), wherein β Com returned to an active phase in the fall months of 1995. Thus, our standard model atmosphere analysis may also be slightly affected – as we have learned from e.g. HD 152391 (see below) – and the Δd=8.3% distance discrepancy may be indicative for that.

59 Vir: this star shows a similar chromospheric activity and discrepant Mg Ib line wings as HD 152391 below. We refer also to the work of Saar & Osten (1997) as well as Radick et al. (1998). From the results of the latter analysis and the fact that the mean rotation period is found to be $\langle P \rangle = 3.33$ days (Donahue, Saar & Baliunas 1996) we conjecture that 59 Vir must be a relatively young (< 1 Gyr) star.

5 Ser: *unlike* other evolved F stars of our sample, 5 Ser shows a consistent gravity determination from the LTE iron ionization equilibrium and the wings of the Mg Ib lines. As such, it is likely that our spectra of this star might be adulterated from binarity or some kind of chromospheric activity. Though existing radial-velocity studies do not provide much evidence to the former possibility (e.g. Abt & Levy 1976, Duquennoy & Mayor 1991), and a qualitative inspection of the cores of Hα and the Ca II infrared triplet is also rather inconclusive with respect to the latter, we should exclude this star from the sample of reliably analyzed stars; this is also implied by comparison with the Hipparcos parallax.

χ Her: the luminosity derived from the Hipparcos parallax immediately gives rise to the suggestion that this standard F9V star must instead be a subgiant. Our spectroscopic analysis confirms this finding with a surface gravity $\log\ g = 3.84$. Compared to the astrometric data there is, however, a Δd=11.2% distance discrepancy, which translates to $\Delta \log\ g = 0.09$ dex, i.e. $\log\ g \sim 3.93$, and this causes some doubts as to whether χ Her is indeed a *single* object. Though this suspicion is not corroborated by existing radial-velocity and speckle observations of this star (e.g. Duquennoy & Mayor 1991, Hartkopf & McAlister 1984), the Hipparcos data present an (albeit questionable) orbital solution. Thus it may also be no coincidence that the Edvardsson et al. (1993) analysis of χ Her (T_{eff}/$\log\ g$/[Fe/H]$= 5843/4.34/-0.52$) shows an unexpected large discrepancy with respect to the derived surface gravity ($\log\ g = 3.84$ vs 4.34), which we have otherwise only found for 99 Her – a well-known visual binary (cf. Paper I, Sect. 4.2). Hence, it appears that the real status of this star still remains to be settled, which is particularly important for χ Her is among the oldest (~ 9 Gyr) and most metal-poor stars of the thin-disk population.

18 Sco: Porto de Mello & da Silva (1997) recently identified this star as *"the closest ever solar twin"* (cf. also Cayrel de Strobel 1996). Our analysis confirms the effective temperature, metallicity, $v\sin i$, and mass to be all indistinguishable from that of the Sun. It is only the surface gravity and bolometric magnitude, and hence the stellar radius, that imply a "Sun" in an advanced stage, approximately 1 Gyr older, compared to our parent star.

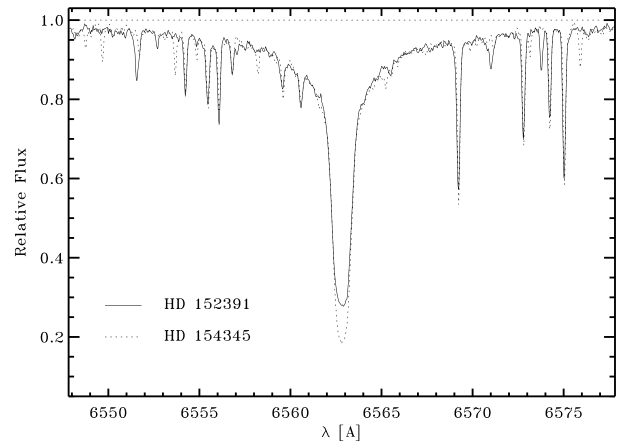

Fig. 9. Comparison of Hα lines of HD 152391 and HD 154345. The partly filled-in line core of HD 152391 is ample evidence for chromospheric activity

ζ Her: this is a nearby visual binary with an orbital period of 34.5 years (cf. Baize 1976). The Hipparcos data give a magnitude difference of 2.68 mag and an angular separation $\rho \sim 1.5$ arcsec. According to the data in Baize (1976) this should have decreased to $\rho \sim 1.1$ arcsec at the time of our spectroscopic observations (June 1998). But, contrary to the case of the binary 99 Her in Paper I where the separation was only a few tenths of an arcsec, we expect that part of the light from the companion of ζ Her was actually lost during our exposures for we made use of a narrow entrance aperture. As a result, it is possible that the brightness contrast even exceeded 4 mag. In any case, we consider the derived stellar parameters to be fairly reliable on account of the good agreement with (i) the Hipparcos distance scale, and (ii) the detailed work by Chmielewski et al. (1995), who additionally modeled the effect of the companion spectrum.

HD 152391: the rare combination of a high space velocity ($U/V/W = 95/-105/17$ km s^{-1}) and strong chromospheric activity is the most astounding feature of this object (cf. Soderblom 1985, 1990). Its status as a BY Dra-type variable implies that is must be either young, or a member of a binary system. Neither case is advantageous for our standard model atmosphere analysis, nor the fact that significant magnetic broadening (which we generally ignore in our analyses) has been found by Saar & Osten (1997, see also Montesinos & Jordan 1993, and references therein). The comparison of Hα and the Ca II infrared triplet with tracings of HD 154345 (which is of similar spectral type, cf. Paper I) clearly demonstrates the existence of filled-in line cores, as illustrated in Figs. 9 and 10.

This however causes doubts as to whether the Balmer lines can be reliable tracers of the effective temperature. LaBonte (1986), for instance, has shown that Hα spectra of solar *plages* not only affect the line cores, but also to a noticeable degree ($\sim$1%) the line wings, which then imply a "lower" effective

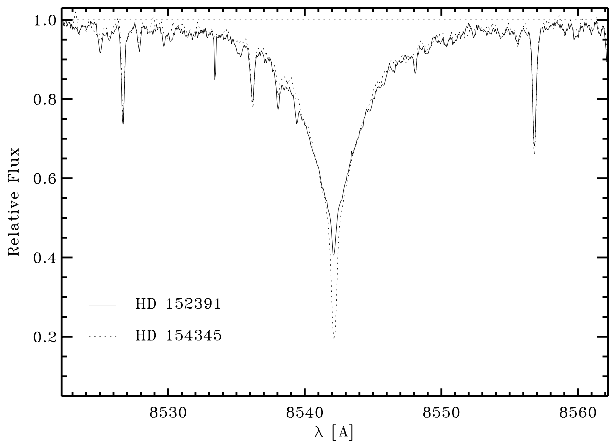

Fig. 10. Same as Fig. 9, but for Ca II λ8542

temperature. Although our spectroscopic analysis, based on the LTE iron ionization equilibrium, results in a perfect agreement with the Hipparcos distance scale, the comparison of the Mg Ib line wings in Fig. 11 reveals a clear inconsistency, which in turn requires an ~ 0.2 dex *decrease* in $\log\ g$. Evidently this must be judged as a strong hint for an erroneous T_{eff} and/or $\log\ g$ (and hence metallicity) in Table 3, and consequently *we have to reject the analysis of this star*. Nevertheless, we feel save to argue that HD 152391 must be a thin-disk star, since there is no signature of a non-solar Fe/Mg abundance *ratio* in the spectra. Likewise, Radick et al. (1998) find for the long-term pattern of Sun-like stars that young, active objects become photometrically fainter as their Ca II H&K chromospheric emission increases. Since HD 152391 sticks to this correlation it should not be older than 1–2 Gyr, where the crossover of that phenomenon occurs. Thus, a peek at the Bottlinger diagram in Fig. 15 (see below) ultimately identifies HD 152391 as a *runaway* star, a point that was already made by Soderblom, Duncan & Johnson in 1991.

HD 165401: in our first analysis of this star in Paper I, HD 165401 was identified as a thick-disk member with an age of about ~ 10 Gyr, whereas all other analyzed thick-disk stars turned out to be older than ~ 12 Gyr. Hence, we considered it worthwhile to re-observe HD 165401 in June 1998, now at $\lambda/\Delta\lambda$ ~60000, and with an improved signal-to-noise. In addition, the employed 2 k CCD covered the Ca II infrared triplet, which was not the case with the older settings in 1995. About the same time we became also aware of HD 165401's conspicuous behaviour that emerged from Soderblom's (1985) work, viz., as a chromospherically active, high-velocity star – a combination that is met for only 4 out of 177 objects in his sample of nearby F to K stars (cf. also Herbig 1985, for the chromospheric Hα emission). Incidentally, HD 152391, another member of this rare group, was also observed in June 1998, and its analysis had to be discarded for the striking discrepancies with the Mg Ib line wings (cf. Fig. 11, and the corresponding notes on HD 152391). The careful reanalysis of HD 165401 revealed that it has indeed similar features as HD 152391, albeit clearly less pronounced, but nevertheless significant. This was, unfortunately, overlooked in the older analysis.

If, however, the measured Fe/Mg deficiency of HD 165401 is real, which we take as indicative for an old object, it is likely to interpret the lasting Ca II activity in terms of binarity. We therefore exclude HD 165401 from the sample of reliable analyses.

ψ^1 *Dra B*: the spectroscopic and astrometric distances deviate by 9%. In this particular case, we notice however an unusual large uncertainty in the Hipparcos data, $\pi = 44.80 \pm 1.94$ mas, i.e. a factor 2-3 higher of what is usually obtained.

HD 184385: this star shares many characteristics with HD 152391. Firstly, the cores of Hα and the Ca II infrared triplet are noticeably filled-in. Secondly, the Mg Ib lines show the same effect as already illustrated in Fig. 11. Thirdly, the LTE iron ionization equilibrium needs an ~ 0.2 dex downward revision in $\log\ g$ (compared to the value of Table 3), which however does not accord with the astrometric distance (Δd~ 35%). We also mention the classification of HD 184385 as an *"uncertain"* candidate, i.e. a suspected spectroscopic binary, according to Duquennoy & Mayor (1991).

15 Sge: as with β Com, we notice slight chromospheric signatures in the cores of Hα and the Ca II infrared triplet, and also a somewhat reduced match with the Mg Ib line wings (cf. HD 152391). Similar to β Com, it also appears that 15 Sge was in an active phase, when we observed this star in June 1998, as implied by the data of Baliunas et al. (1995).

5. Implications for the Galaxy

5.1. *Identity of the field stars*

Along with the data of Paper I and the results of the preceding section we begin the discussion of the relevant items for the Milky Way Galaxy with the for that purpose central Fig. 12. Herein abundance ratios of iron and magnesium are presented as a function of the overall metal content, measured as either [Fe/H] or [Mg/H]. In combination with age estimates from stellar evolutionary tracks and the kinematical properties of the stars the fairly reliable identification of the *individual* stars in terms of halo, thick-disk and thin-disk population was suggested in Paper I. *The comparison with the corresponding Fig. 11 of that paper now shows that the basic characteristics actually remain unchanged.* Thus the reader is referred to the original discussion of Paper I. It is only two additional points that we must address here: firstly, most of the newcomers in Fig. 12 are also objects of the Gliese & Jahreiß CNS4 Catalogue. In fact, and as we discuss below, our sample contains by now approximately *one-third of all F5 to G9, as well as evolved K stars, within 25 pc and north of a declination of* $-15^{\rm o}$. Yet, HR 4098 and ρ CrB at 23.6 pc and 17.4 pc, respectively, are the only "transition stars" within 25 pc (the third object in Fig. 12, HR 7569, is at a distance of 27.7 pc). In other words, the transition region defined by these three stars is very likely a poorly populated one.

Secondly, for the discussion of the discreteness of the two *disk* populations it is clear that they reveal a considerable

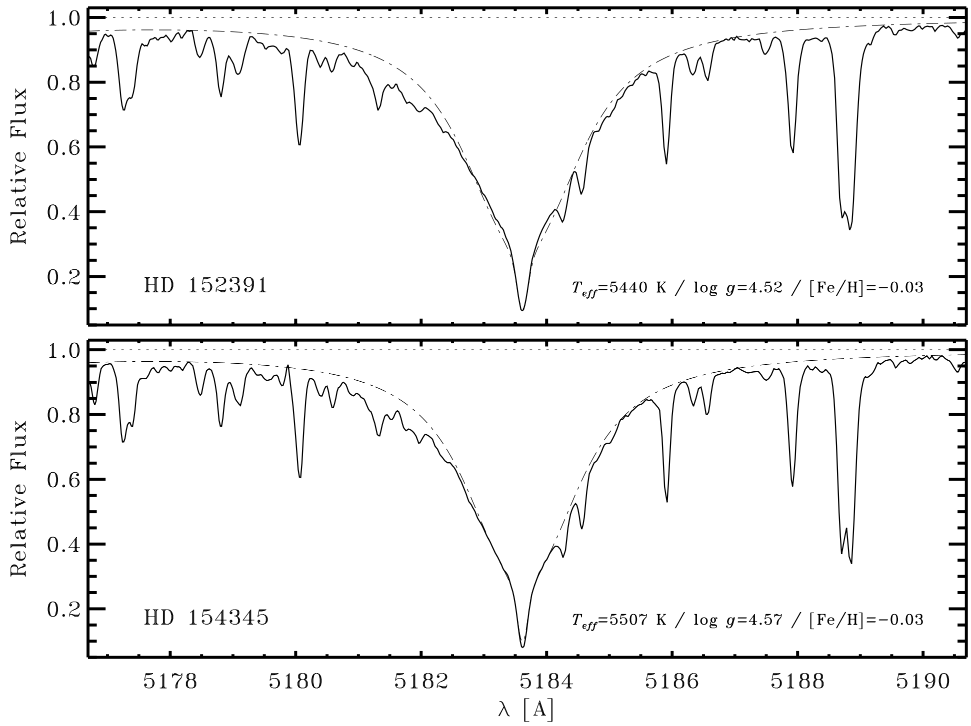

Fig. 11. Line profile analysis of the Mg Ib line λ5183 for HD 152391 and HD 154345. The theoretical calculations refer to the LTE iron ionization equilibrium and result in a perfect match for HD 154345, but a clearly discrepant case for HD 152391. A *decrease* in $\log\ g$ by $\sim\ 0.2$ dex is required for the latter, which is however at variance with the Hipparcos parallax

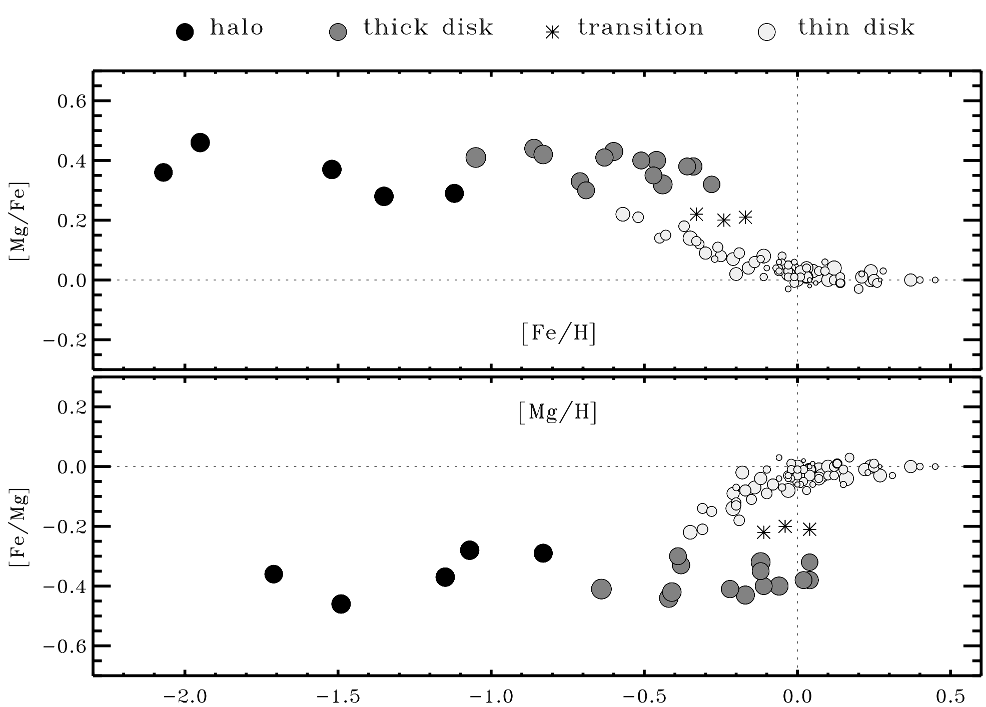

Fig. 12. Top: abundance ratio [Mg/Fe] versus [Fe/H]. Bottom: the same data, but with magnesium as reference element. Except for the three “transition stars” (given by asterisks), depicted circle diameters denote age estimates, with small diameters indicating the youngest stars. Different *stellar populations* are given with various grayscale symbols as indicated in the legend on top, and are based on abundance, kinematics and age informations (see text for details)

abundance overlap between thick- and thin-disk stars, especially with the Mg abscissa in the lower panel of Fig. 12. Although this degeneracy is considerably relaxed with reference to the depicted *abundance planes*, there is nevertheless a region, where thick- and thin-disk stars come *chemically* very close to each other. In addition (as we will see below), there is also some *kinematical* overlap with the disk populations. It is therefore important to realize that the key feature to identify thick- and thin-disk stars individually is provided by the *stellar ages*: all the thin-disk stars of Fig. 12 with meaningful age de-

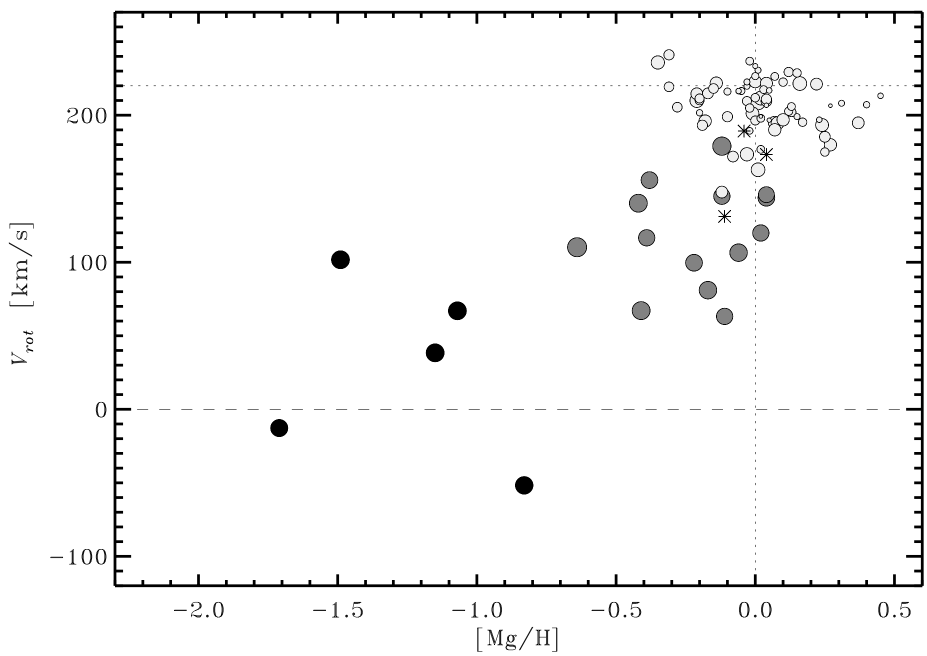

Fig. 13. Galactic rotational velocity $V_{rot} = V + 220$ km s^{-1} versus metallicity. The dashed line separates prograde and retrograde rotation. Grayscaling and symbol sizes have the same meaning as in Fig. 12

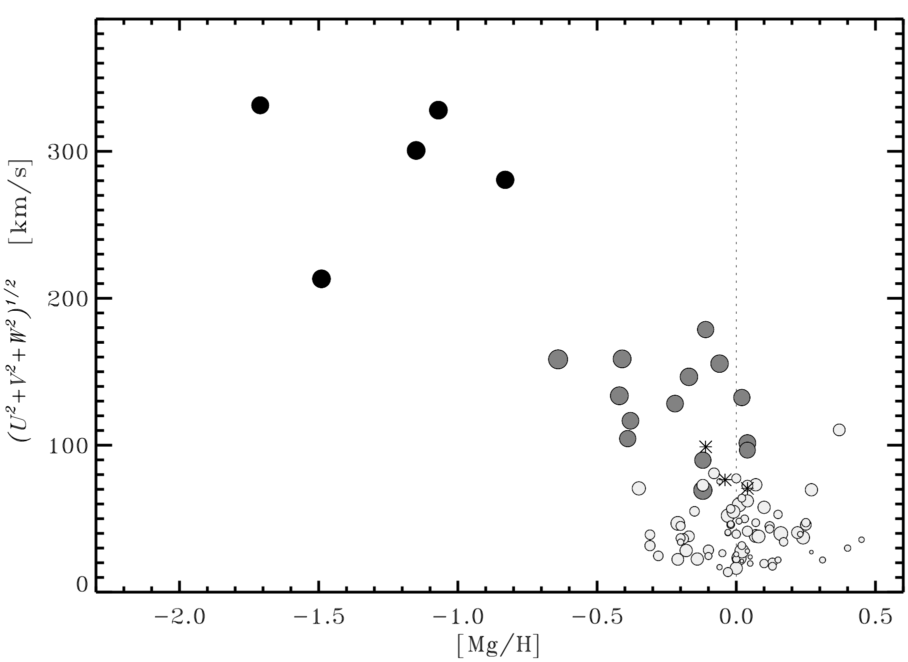

Fig. 14. Peculiar space velocities $v_{pec} = (U^2 + V^2 + W^2)^{1/2}$ versus metallicity. Grayscaling and symbol sizes have the same meaning as in Fig. 12

terminations (i.e. excluding the colder objects on the main sequence) do not exceed ~ 9 Gyr, whereas with the exclusion of the chromospherically active HD 165401 (cf. Sect. 4.2) all analyzed thick-disk stars stick to a lower limit of ~ 12 Gyr (again, unevolved stars, like μ Cas at $T_{eff} = 5387$ K, are irrelevant). That is, the data of Fig. 12 *now* suggest a reduced rate or even a hiatus in star formation of about *three billion years*[3]. Within that intermediate phase at least two of the three identified transition stars, ρ CrB and HR 7569, rather define the *onset of the thin disk*, than the end of the thick disk, as we will also show later with the stars' kinematics.

With respect to the separability of halo and thick-disk stars, there is neither a case for chemistry (in terms of Mg or Fe) nor age as for the disk populations. Although halo stars are thought

[3] we note in passing that age determinations of nearby *field* stars can in fact be very accurate in the Hipparcos era, in particular for stars on the subgiant branch as has recently been demonstrated by Dravins, Lindegren & VandenBerg (1998)

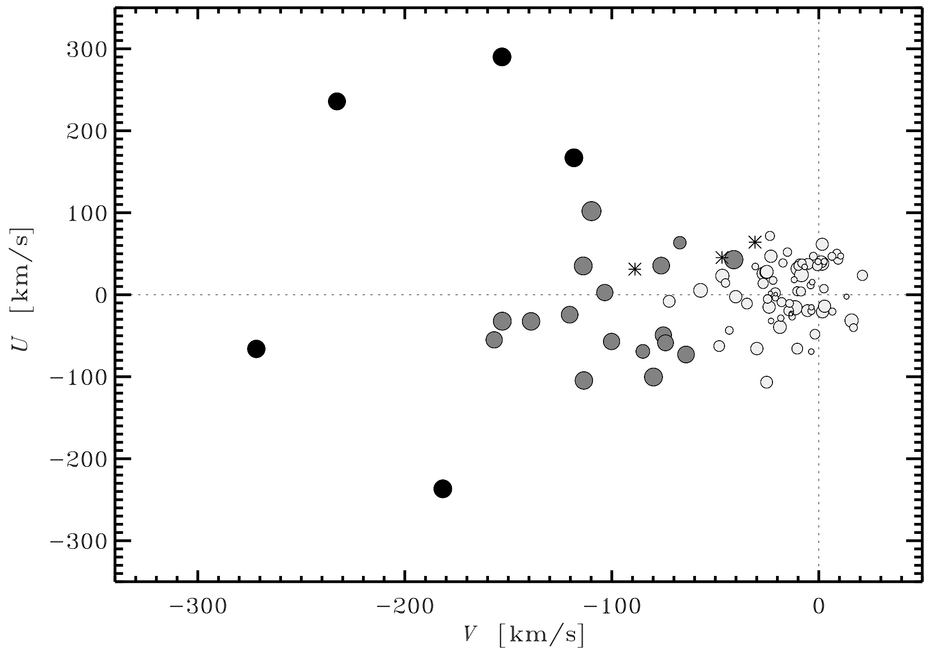

Fig. 15. Bottlinger diagram: U versus V velocities. Grayscaling and symbol sizes have the same meaning as in Fig. 12. Note that the thick-disk stars Arcturus, HR 4657, and HD 165401 are also included

of to be generally more metal-poor, a considerable abundance overlap with thick-disk stars is discussed in the literature (the so-called "metal-weak thick-disk stars") and from our sample we learn also about common abundance ratios and ages. Evidently then, the *kinematics* of the halo and thick-disk stars must be rather distinct, and, indeed, as we will see below it is predominantly this characteristic that allows for our sample to decide which stars belong to the halo and which to the thick disk.

We now turn to the kinematical aspects of the analyzed stars. Since most of the sample stars are very nearby, their phase space data are usually very well known. Typical uncertainties in the space velocities are ~ 1 km s^{-1} and most of the data on the kinematics that we present can be downloaded via http://www.ari.uni-heidelberg.de/aricns/. The correction for the basic solar motion which we adopt is that of Dehnen & Binney (1998), namely, $U_o/V_o/W_o = 10.00/5.25/7.17$ km s^{-1}.

Fig. 13 compares the stars' Galactic rotational velocities $V_{rot} = V + 220$ km s^{-1} and Fig. 14 their peculiar space velocities $v_{pec} = (U^2 + V^2 + W^2)^{1/2}$, both as a function of stellar metallicity. In each case there is a clear gap between halo stars and thick-disk stars, which confirms their distinctness (cf. also the corresponding diagrams in Schuster, Parrao & Contreras Martínez 1993, and Carney et al. 1996, for much larger samples). Particularly remarkable in our work however is the rather unexpected weak kinematical overlap of the disk populations. We measure a mean Galactic rotational velocity $\langle V_{rot}\rangle = 122$ km s^{-1} for our admittedly small (N=17) and certainly not representative sample of thick-disk stars, which corresponds to an asymmetric drift velocity of no less than $\langle \Delta V_{rot}\rangle \sim -80$ km s^{-1} relative to the "old" thin disk (arbitrarily defined here in terms of stars with a minimum age of $\sim$4 Gyr).

From a comparison of the extensive literature that exists on this issue it is interesting to see that our finding for a well-distinguished drift velocity of the thick disk is clearly at variance with most of the analyses that have been published to date and which cluster around $\langle \Delta V_{rot}\rangle \sim -30... - 50$ km s^{-1} with respect to the local standard of rest (e.g. Sandage & Fouts 1987, Carney, Latham & Laird 1989, Soubiran 1993, Ojha et al. 1994, Beers & Sommer-Larsen 1995, Ojha et al. 1996, Norris 1999). Our value is however in good agreement with the very recent spectroscopic work of Chen et al. (2000), and, in particular, agrees with the early measurements of Wyse & Gilmore (1986). It is thus basically a resurgence of the early picture that was advocated by Gilmore, Reid and Wyse in the 1980s.

Purely kinematical diagrams of our sample are displayed in Fig. 15 (U vs V), Fig. 16 (W vs V), and the Toomre diagram of Fig. 17. The latter suggests a peculiar space velocity $v_{pec} \sim 85$ km s^{-1} as a useful discrimination for thick- and thin-disk stars. The only two exceptional cases in Fig. 17 are the thick-disk object HD 37124 ($v_{pec} = 69$ km s^{-1}) and the super-metal-rich star 31 Aql. The latter has an extreme U component ($U = -107$ km s^{-1}) which is suggestive of a connection to the Galactic *bulge*, as has earlier been proposed by e.g. Grenon (1999). Fig. 17 also indicates that an orbital rotational velocity $V < -40$ km s^{-1} may be another appropriate criterion in a search for thick-disk stars. Along with the above $v_{pec} \sim 85$ km s^{-1} threshold for the total space velocity this might in fact be a very efficient combination to pre-select many *candidate* thick-disk stars.

As a cautionary remark on the small number of the thick-disk and halo stars in our sample, we mention that from inspection of the U vs V Bottlinger diagram in Fig. 15 one may notice a predominance of negative U velocities, i.e. towards the Galactic anticenter, for the 17 depicted *thick-disk* stars.

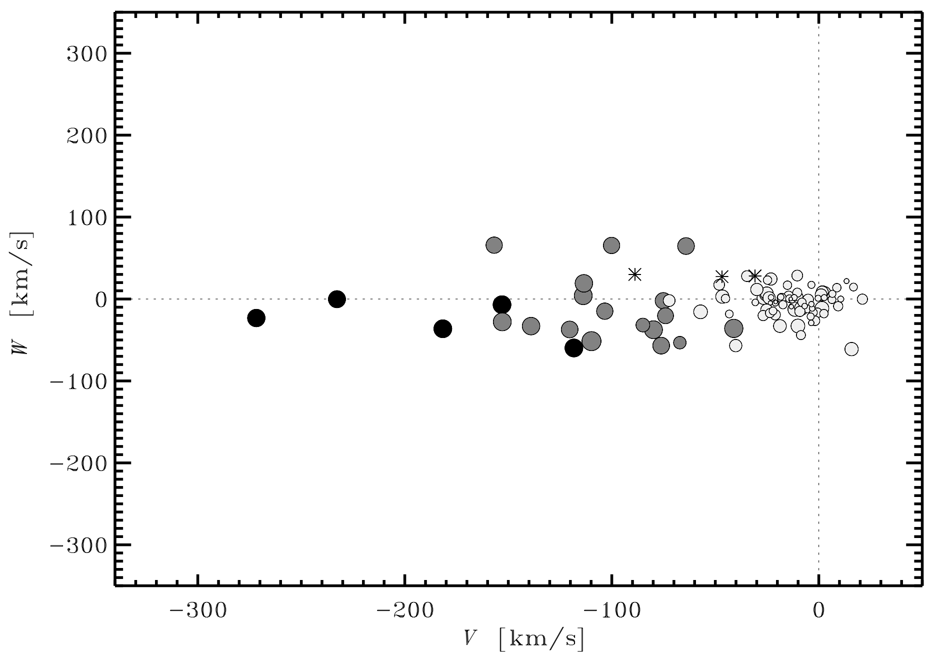

Fig. 16. V-W diagram. Grayscaling and symbol sizes have the same meaning as in Fig. 12. Note that the thick-disk stars Arcturus, HR 4657, and HD 165401 are also included

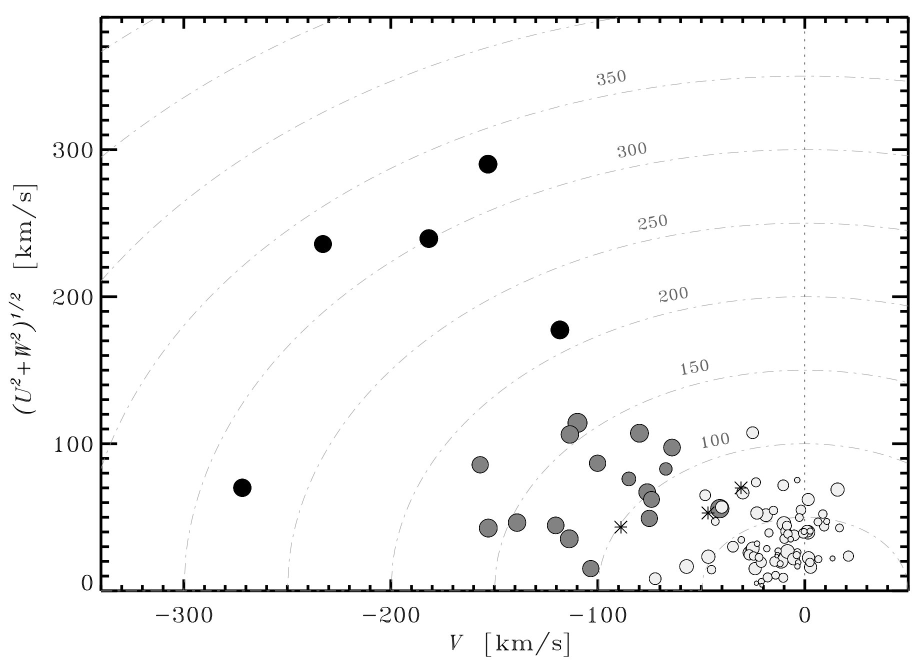

Fig. 17. Toomre diagram from the perspective of the local standard of rest. Circles delineate constant peculiar space velocities $v_{pec} = (U^2 + V^2 + W^2)^{1/2}$ in steps of $\Delta v_{pec} = 50$ km s^{-1}. Except for HD 37124 ($U/V/W = 43/-41/-36$ km s^{-1}), the thick-disk stars of this sample are found in the interval 85 km s^{-1} $< v_{pec} <$ 180 km s^{-1}. Grayscaling and symbol sizes have the same meaning as in Fig. 12. Note that the thick-disk stars Arcturus, HR 4657, and HD 165401 are also included

Their average $\langle U \rangle = -22$ km s^{-1} is however to compared with the velocity dispersion $\sigma_U = 59$ km s^{-1}. Similarly, the small dispersion of the W velocities for the few halo stars in Fig. 16 would not show up for larger sample of these objects (cf. Jahreiß, Fuchs & Wielen 1997).

Coming back to the transitions stars ρ CrB ($U/V/W = 64/-31/28$ km s^{-1}) and HR 7569 ($U/V/W = 45/-47/27$ km s^{-1}), we register similar characteristics for both in Figs. 13 through 17, which implies a common origin. As already mentioned above, their space motions are evidently best described as a hot *thin-disk* kinematics. It is only HR 4098 ($U/V/W = 31/-89/30$ km s^{-1}) that shows thick-disk kinematics, at variance with its chemistry and age.

One additional feature of the kinematics of our sample merits mention. Among the identified thick-disk stars, HR 4657 (cf. Fuhrmann & Bernkopf 1999), HD 62301, HD 204155, and

HD 221830 have previously been classified by Eggen (1971, 1998a,b) as members of the "Arcturus Group". In fact, Eggen proposed a mean $V = -110$ km s^{-1}, i.e. not very different from ours for the thick disk, and a comparison of our thick-disk rotational velocity dispersion $\sigma_V = 32$ km s^{-1} is in very good agreement with the Hipparcos-based value $\sigma_V = 30$ km s^{-1} for the "Arcturus Group" given by Skuljan, Cottrell & Hearnshaw (1997). In a comparative study of Eggen's moving groups these authors however notice that *"the Arcturus Group covers a large portion of the UV plane, and does not look like a moving group at all"*. Indeed, our work readily suggests that what Eggen called the "Arcturus Group" is most likely the manifestation of the *local* thick disk, with Arcturus now as its principal agent.

5.2. A volume-limited sample

So far we have paid closest attention to describe criteria for an unequivocal distinction of the halo, thick-disk and thin-disk population. With the ability for a fairly reliable identification of the individual stars, it is now tempting to define meaningful samples for a more detailed study of the formation and evolution of the Milky Way Galaxy. One particularly suited sample is the classical volume-limited inventory of F, G, or K stars within 25 pc (cf. van den Bergh 1962, Pagel & Patchett 1975, Wyse & Gilmore 1995, Rocha-Pinto & Maciel 1996, Haywood et al. 1997, Favata, Micela & Sciortino 1997, Flynn & Morell 1997). Though the sampled region is extremely tiny, it allows one to work with detailed information on parallaxes, kinematics, spectroscopic binaries, etc. Thus our interest is not only restricted to halo and thick-disk stars, but also to include all nearby F/G stars (as well as the few evolved K stars) within 25 pc. Since, however, the observations are conducted from the Calar Alto Observatory in the northern hemisphere, we loose the stars south of $\delta = -15^{\rm o}$, which is about 1/3 of the sky.

Next we define in more detail the projected T_{eff}-$\log g$ parameter space for the volume-limited sample. First of all, we include the complete set of G-type stars of luminosity class IV and V, which corresponds to a lower limit in effective temperature of $T_{eff} \sim$ 5200-5300 K on the main sequence *at solar metallicity*. The spectral classification of metal-poor stars is however known to be notoriously too early, and, vice versa, that of the metal-rich stars usually too late. Thus it happens that the only CNS4 halo star of our sample, HR 4550 (=Gmb 1830, G8VI) at $T_{eff} = 5110$ K (cf. Paper I), is better characterized as a K star. 14 Her, on the other hand, the most metal-rich star of the up to now analyzed sample is classified as K0V, but comes out with $T_{eff} = 5334$ K, i.e. rather mimics a late G-type star. Therefore, to make sure that we are complete in this range of the main sequence, we adopt $T_{eff} = 5400$ K as a lower limit.

One may argue that it might be better to define a lower *mass* limit for the stars on the main sequence, but then one faces the problem that metal-rich stars at the transition from spectral types G to K (e.g. ρ^1 Cnc, 14 Her) are already above $1 M_\odot$ (cf. Fig. 7, in particular with respect to the neighboring μ Cas), whereas all thick-disk F/G stars of $1 M_\odot$ have experienced hydrogen exhaustion for a long time. A solution might be to proceed to even cooler stars on the main sequence, but this then involves a much larger sample, which is beyond the scope of the present project. For main-sequence stars below $T_{eff} = 5400$ K it is also progressively difficult to derive meaningful, if any, age estimates from stellar evolutionary tracks. Thus our primary criterion to distinguish thick- and thin-disk stars gets lost. As a result, it is rather the light (luminosity) than the dark (mass) aspect of the stars that is compared by introducing the $T_{eff} = 5400$ K lower main-sequence cut.

Table 4. Space velocities of the giants within 25 pc and north of $\delta = -15^{\rm o}$. In the last column, $v_{pec} = (U^2 + V^2 + W^2)^{1/2}$ is the peculiar space velocity of the stars

Object	HR	Sp. Type	U [km/s]	V [km/s]	W [km/s]	v_{pec} [km/s]
α Ari	617	K2III	10	–22	10	26
Aldebaran	1457	K5III	–38	–13	–18	44
Capella Aa	1708	G5IIIe	–26	–9	–2	28
Capella Ab	1708	G0III	–26	–9	–2	28
Pollux	2990	K0IIIvar	–6	10	–19	22
Arcturus A	5340	K2IIIp	35	–114	4	119
Arcturus B	5340		35	–114	4	119
α Ser	5854	K2III	16	19	2	24
η Ser	6869	K0III-IV	54	–60	23	84
ϵ Cyg	7949	K0III	–42	6	0	42

For the cool *evolved* stars below $T_{eff} = 5400$ K we restrict the model atmosphere analyses to those with $\log g \geq 3.0$, which also causes the inclusion of a handful of K subgiants.

In addition, we consider the few existing nearby giant stars with respect to their kinematics and, hence, possible population membership in the star-count analysis. They are given in Table 4. Application of the $v_{pec} > 85$ km s^{-1} criterion shows that it is only Arcturus which possesses thick-disk kinematics, although η Ser must be considered as another possible candidate. With reference to Edvardsson's (1988) careful spectroscopic analysis we note however that, while Arcturus shows the typical thick-disk Fe/Mg underabundance, this is not the case for η Ser, which ties in with a thin-disk membership for this star.

As far as the F stars are concerned, it is well-known that metal-poor stars can reach up to $T_{eff} \sim 6500$ K at the turnoff. This corresponds to ~F5 for solar-type stars and is also the region where a steep increase of stellar rotational velocities is known to take place (e.g. Kraft 1967). Projected rotational velocities in excess of $v\sin i \sim 20$ km s^{-1} usually prohibit the study of unblended line profiles and thereby a reliable surface gravity determination, which, in our case, depends to a large extent on the availability of the weak Mg I lines λ4571 and λ5711 (to fix the abundance of the Mg Ib triplet). Here we will therefore restrict the analyses to stars later than ~F5, $v\sin i \leq 20$ km s^{-1}, and luminosity classes IV and V (actually there are no F5 to F9 giants within 25 pc and north of $\delta = -15^{\rm o}$). Up to now only four nearby thin-disk stars (not

Table 5. Nearby F-type stars with $v\sin i > 20$ km s^{-1}. These have been excluded from a thorough spectroscopic analysis. The tabulated effective temperatures represent only crude estimates from the Balmer lines, whereas the surface gravities utilize the Hipparcos parallaxes

Object	HR	HD	T_{eff} [K]	$\log g$ [cgs]	ζ_{RT} [km/s]	$v\sin i$ [km/s]
	4867	111456	6300	4.32	5.7	41.0
θ Boo	5404	126660	6200	4.02	6.0	29.5
45 Boo	5634	134083	6480	4.30	6.4	45.0
θ Dra	5986	144284	6140	3.77	6.1	28.5

included in Fig. 5) with $v\sin i > 20$ km s^{-1} entered our sample. We tabulate provisional effective temperatures, Hipparcos-based surface gravities, (adopted) macroturbulence velocities and measured $v\sin i$'s of these objects in Table 5. Note that both stars with $v\sin i > 40$ km s^{-1}, HR 4867 and 45 Boo, are members of the young Ursa Major Cluster ($\tau \sim 0.3$ Gyr).

We now ask: how many of the so-defined F and G dwarfs and subgiants are to be found in the CNS4 Catalogue? To answer this question it must first be realized that our $T_{eff} \geq 5400$ K criterion for the main sequence is applicable only *a posteriori.* Another uncertainty is that some objects are binary candidates, and some of the stars are the *secondaries* around hotter stars (e.g. α CrB, β Ari, τ Cyg, 78 UMa, ι Leo). An additional concern results from the members of the Ursa Major Cluster. Should one consider these objects in a representative sample of *field* stars? Fortunately it seems that there is only a handful of these objects in our temperature range within 25 pc.

Thus our counting has some restrictions, but we expect about ∼80 F5-F9 dwarfs and another ∼160 G dwarfs within 25 pc, north of $\delta = -15°$, and with $T_{eff} \geq 5400$ K on the main sequence. To them we add the few existing nearby K subgiants as well as the G/K giants of Table 4.

A very important question is then: how many of the already analyzed CNS4 F5 to K sample stars belong to the thick disk, and how many will ultimately enter the complete sample? With final results for about one-third of the stars of our volume-limited CNS4 sample the answer to the first part of the question is “5 stars”, namely, HD 18757, HD 22879, 72 Her, HD 165401, and the putative *blue straggler* HR 4657. For the second part of the question we apply the $v_{pec} > 85$ km s^{-1} criterion inferred from Fig. 17, which gives rise to another 2–4 stars. (A *complete* account of the local thick-disk stars will be given in part III of this series.) A special case is that of Arcturus, where – quite unexpected – a faint companion was recently discovered by Hipparcos. With a given magnitude difference of 3.33 mag this is most likely a subgiant of $T_{eff} \sim 5000$ K and $\log g \sim 3.3$, but there are also some oddities with “Arcturus as a double star” that have duely been pointed out by Griffin (1998). But for the time being we have to include *both* in the star-count analysis as thick-disk members. We note in passing that it is already clear by now that none of the so-called *metal-weak thick-disk stars* will enter our – admittedly small – sample.

Finally, recall that there is *no* halo star in our above defined CNS4 sample.

5.3. The census of long-lived stars

Thus we count ∼10 stars for the thick disk and some ∼240 stars for the thin disk. That is, about 4% of the *local* F5 to G9, as well as evolved K stars, are thick-disk stars. Adopting double-exponential density laws for both disk populations with ratios 1000 pc:250 pc for the scale heights and 4 kpc:3 kpc for their scale lengths[4] (see e.g. Sackett 1997, Norris 1999, for some references), this results in a fraction of ∼15% for the thick-disk stars in total.

This rough estimate involves however a crucial mistake: since it must be our interest to compare the number of *all ever formed* thick-disk F- and G-type stars to that of its thin-disk congeners, we have to realize that all the thick-disk objects that we see today in this temperature range are rather the tip of an iceberg. To understand this assertion quantitatively we explicitly inquire: *how many stars of our thin-disk sample are actually long-lived?* If we adopt ∼14 Gyr as a reasonable limit for a long-lived star, it turns out (cf. Fig. 18) that we have to discard *all* F stars of the thin disk (ironically it is the *thick disk* that possesses two long-lived F stars. One is the above mentioned blue straggler candidate HR 4657. The other, HD 22789, is misclassified as “F9V” as a result of its reduced metallicity). Though this result is certainly not unexpected, it is the G stars that are found something of a surprise: while it is usually taken for granted that the bulk of G-type stars may easily reach the age of the Galaxy (but often without stating what this *explicitly* means), a preliminary estimate on the base of our up to now analyzed G stars suggests that *only about one-third of the 160 G stars with T_{eff} ≥5400 K is actually long-lived*, i.e. will reach an age of 14 Gyr before a transition to the white dwarf regime takes place. Likewise, we have to exclude with this rating the thin-disk G/K giants of Table 4 (all stars except for Arcturus), because with an upper limit of ∼9 Gyr for the thin-disk population, *all* these evolved stars are inevitably short-lived. As a result, the fraction of *local* long-lived thick-disk versus thin-disk stars is

$$\mathrm{N}_{thick} : \mathrm{N}_{(thin+thick)} \approx 10 : 60 \approx 17\%,$$

and, consequently, the *total* mass of the thick disk – adopting the above given vertical and radial scale-height ratios and an invariant initial mass function – might then be *comparable to that of the thin disk!*

Is this then a case for a *maximal* disk for the Milky Way as discussed in Larson (1986) and, more recently, by Sackett

[4] the scale length of the thick disk is certainly the least constrained. But in view of the fact that our individually identified thick-disk stars show a pronounced rotational lag, a scale length 1 kpc in excess of the adopted 3 kpc for the thin disk is presumably a conservative *lower* limit for the thick disk

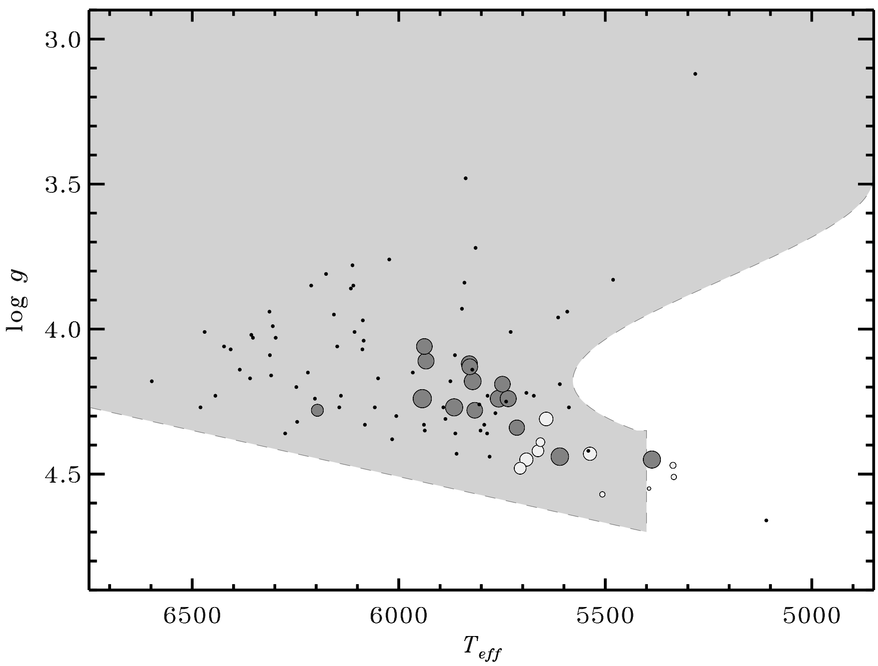

Fig. 18. *Kiel diagram* of the long-lived *disk* stars. The stars of the thick disk are long-lived by definition. Their reduced metal abundance causes a shift of the corresponding turnoff positions to hotter effective temperatures. The fact that most of the given thick-disk stars cluster around the turnoff is a selection effect (nearby thick-disk stars are rare and the brightest most likely to be found at the turnoff). The hot maverick to the left is the *blue straggler* candidate HR 4657. The position of Arcturus is far-off the displayed parameter range. Its putative companion however might lie in the upper right corner (T_{eff}/$\log g$ $\sim$ $5000/3.3$). Grayscaling and symbol sizes have the same meaning as in Fig. 12, except for the small black dots, which depict the position of either halo or short-lived disk stars. Shading indicates the selected region of the volume-limited sample, with T_{eff} $=$ 5400 K taken as the lower limit on the main sequence (note that the unevolved thick-disk star μ Cas, T_{eff} $=$ 5387 K, falls short of this value)

(1997), but at variance with the findings of e.g. Kuijken (1995), Crézé et al. (1998), and Méra, Chabrier & Schaeffer (1998)? Certainly, several cautionary remarks on a massive thick disk are to put forward, the first being, that the above suggested 1:1 mass ratio of the disk populations is currently an *extrapolation* on the base of only one-third of the analyzed stars of a small volume-limited sample. Then, it is already clear *by now* that, unfortunately, the data on the Galactic thick-disk component within 25 pc will finally represent a low-number statistics. Furthermore, the above mass budget integrates down to M $\sim$0.8 $M_\odot$ for thick-disk stars with $\langle$ [Fe/H] $\rangle$ ~ -0.6, compared to only M $\sim$0.9 $M_\odot$ for the thin disk at solar [Fe/H], and, no less important, there are uncertainties in the disks' scale heights and lengths, as illustrated in Fig. 19. For the thin disk, with a much longer *timespan* of star formation, the adopted 250 pc scale height is inevitably a crude compromise in response to the time-dependent vertical disk heating. Pham (1997), for instance, reports a substantially minor 165 pc height on the base of a Hipparcos F star sample, with ages mostly below 4 Gyr. With respect to the thick-disk component, we have already mentioned its uncertain scale length, but there is also a considerable range of scale heights in the literature ($\sim$600...1500 pc).

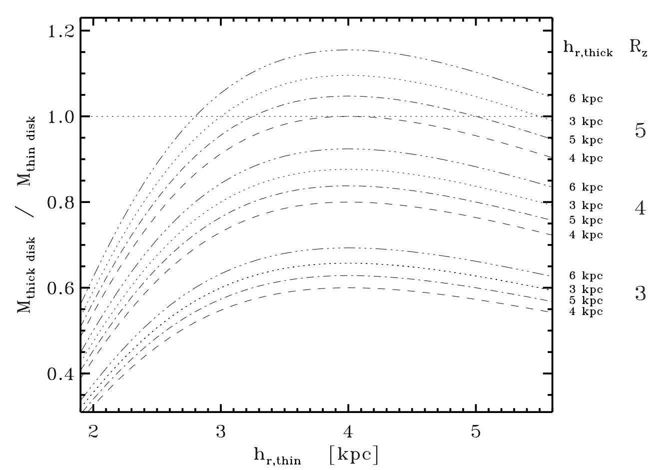

Fig. 19. Ratio of exponential disk masses $M \sim 4\pi\rho_\odot h_z e^{R_\odot/h_r} h_r^2$ as a function of the thin-disk scale length $h_{r,thin}$, and for various thick-disk scale lengths $h_{r,thick}$ and scale-height ratios R_z (indicated in the legend). $R_\odot$ $=$ 8 kpc is the adopted distance to the Galactic center. The local disk volume mass density ratio $\rho_{\odot,thick}/\rho_{\odot,thin}$ is given by N_{thick} : $\mathrm{N}_{thin} = 10 : 50 = 0.2$. The three depicted bundles refer to scale-height ratios $R_z = h_{z,thick}/h_{z,thin} = 5, 4, 3$ (top to bottom)

The presumably most important aspect on the mass of the thick disk may however arise from the recent work of Favata, Micela & Sciortino (1997). Herein the authors present spectroscopic analyses of a volume-limited sample of 91 nearby G and K dwarfs with the surprising finding that *none* of their objects below T_{eff} $\sim$ 5100 K is actually metal-poor! On closer inspection of their Fig. 1 and with the background information from our analyses, one readily wonders whether thick-disk stars generally possess a mass cut at $\sim$0.7 $M_\odot$. Should this turn out to be true[5], it would *considerably reduce* our above

[5] we note in passing that another piece of evidence for the suggested thick-disk mass cut comes from the local stellar luminosity function (cf. Jahreiß & Wielen 1997). Herein the thick-disk stars are manifested

given thick-disk mass contribution. But, on the other hand, this would inevitably also cause a severe constraint on the involved *initial mass function* and challenge anyone's conviction in its universality. It is thus tempting to ask: is the mass cut, if real, ultimately a clue or even an imprint for a high- or intermediate-mass-biased initial mass distribution of the thick disk, in a manner as described in e.g. Schwarzschild & Spitzer (1953), Larson (1986), or, more recently, Chabrier, Segretain & Méra (1996) and Fields, Mathews & Schramm (1997)? [6] And does this then entail that the thick disk formed substantially *more* massive stars than the thin disk ever did? As we will see in the next subsection this may in fact be the case.

Coming back to the unevolved low-mass stars, a straight test to get some more hints on the disks' mass budget of these objects would be to study the velocity space of nearby mid- to late-K stars, which should be cooler than the critical $T_{eff} \sim 5100$ K: on the base of e.g. classified K5V stars in the Hipparcos Catalogue there should be about 20% of them with thick-disk kinematics (i.e. with $v_{pec} > 85$ km s^{-1}), *if* we adopt an invariant initial mass function for both disk populations.

Actually what we find is only $\sim 10\%$ for an all-sky sample of 133 K5V stars in the Hipparcos Catalogue within 50 pc. For comparison, we also selected a related set of 199 G5V stars and get $\sim 12\%$ of stars with $v_{pec} > 85$ km s^{-1}. For the latter sample we must however first correct for the contribution of thin-disk G5V stars that cannot be treated as long-lived. This might raise the relative fraction of these local thick-disk stars by a factor of two. If then, we take into account that part of the high-velocity stars should inevitably be thin-disk outliers we might finally arrive at ∼20% for the fraction of local long-lived thick-disk G5V stars. For the K5V star sample, all objects are without exception long-lived, and with the same assumption on the existence of a few thin-disk high-velocity stars the fraction of thick-disk K5V stars may be significantly less than ∼10%. Note also that the selected K star sample is evidently *not* volume-complete (133 K5V vs 199 G5V stars), and therefore most likely biased towards high-velocity stars, i.e. even a fraction of, say, ∼5% thick-disk K5V stars might be taken as an upper limit for the lower main sequence.

Thus, one might in fact argue for a general sparseness of low-mass ($\lesssim 0.7\ M_{\odot}$) thick-disk stars. We note however that without further *spectroscopic* confirmation these estimates on the base of the selected G5V and K5V datasets must be considered highly uncertain at present.

with a fraction of ∼8% in the $M_V = 5$ and $M_V = 6$ bins, and thus produce part of the observed "hump", whereas at $M_V = 7$ there is the well-known "Wielen dip" (which is thereby *not* solely the result of stellar physics, as has been claimed earlier; cf. Kroupa, Tout & Gilmore 1993)

[6] note however that only Larson explicitly argues with a thick disk: "*All of the unseen mass within the Holmberg radii of spiral galaxies could be in remnants if the remnants occupy a thicker disc than the visible stars.*"

5.4. The lost population: stellar remnants in the backyard

With respect to the production rate of the thick-disk F- and G-type stars in the early Galactic epoch our argumentation is however more concise. From the above given local star counts and the disk scale-height and scale-length ratios we readily deduce for the ∼1-2 Gyr thick-disk star formation phase a production of as many F/G stars (and presumably hotter stars as well) as we observe for the subsequent ∼9 Gyr timespan of the thin disk.

Thus one is led to a picture wherein a relatively short phase of vivid star formation in the early Milky Way Galaxy came to a more or less self-regulated ending from the consumption and/or disruption of gas via injection of momentum and energy from massive stars. Recall that in Fig. 12 all thick-disk stars have an Fe/Mg deficiency, that, again, illustrates the short timescale of the first disk star formation phase. The fact that some of these ancient stars formed in surroundings enriched to even *solar* magnesium abundances is a clear indication for a high activity of star formation at that time. Even more, the remarkably high *mean* abundances, $\langle$ [Fe/H] $\rangle = -0.59$ and $\langle$ [Mg/H] $\rangle = -0.21$, of the thick-disk stars witness the large amount of mass that must have been involved in that phase.

Hence, the thick-disk population is certainly not a tiny appendage, "a nice detail" so to speak, for Galactic evolution studies, but instead one of the *key* features without which the history of our Milky Way is simply not traceable.

But if, as we state, the thick disk was – long before the "familiar" Milky Way came on stage – the brilliant firework display in the sky, with the number of all ever formed (bright) stars comparable to – or even exceeding – that of the thin disk, and if, many of the thick-disk stars have since surpassed the relatively short phase in which we currently see K stars like Arcturus struggling, *then there must be a fair number of dim stellar remnants in the Galactic halo observable.* This may indeed be the case, since the recent microlensing measurements along the line of sight to the Large Magellanic Cloud (Alcock et al. 1997) favour the existence of white dwarfs for the Galactic dark halo, *provided* they are very old[7] (cf. Tamanaha et al. 1990, Chabrier, Segretain & Méra 1996, Graff, Laughlin & Freese 1998, Chabrier 1999). This is, of course, not to say that *all* white dwarfs of the halo have their origin in the thick-disk population. But it is nevertheless reassuring to see that what we claim to exist in the Galactic backyard, has a very likely counterpart in the observed microlensing events.

From the suggested 1:1 thick disk – thin disk mass ratio (adopting alike initial mass functions) for at least the "upper" main sequence (i.e. $M >\sim 0.7\ M_{\odot}$), one should expect the thick disk – being the substantially older population – to *outnumber* the inventory of white dwarfs of the thin disk. It then follows that we may have a dim and sparse population of no less than $\sim 2-3 \times 10^{10}$ thick-disk white dwarfs lurking in the Galaxy. As such they certainly provide far more than the 1% contribution to the observed massive compact halo ob-

[7] but see also Hansen (1998) for the existence of old and *blue* white dwarfs

jects, as assessed by Alcock et al. (1997). But, should there have been a bias towards high- or intermediate-mass stars in the initial mass function of the thick disk, as is indicative from the disk populations' star-formation gap, or the putative low-mass cut at $\sim 0.7 M_\odot$, the real amount of Galactic thick-disk white dwarfs may easily exceed the above given number. If so, they would give rise to a remnant-dominated thick-disk population. Keeping in mind that our long-lived thick-disk stars probe only a small mass interval $0.75\ M_\odot < M < 0.95\ M_\odot$, an early stage wherein even $\sim 10^{11}$ thick-disk higher mass stars burnt to white dwarfs is then indeed a possible scenario. Perhaps not only in this case part of the deposits might have been removed through a galactic wind to the intergalactic medium as recently described in Fields, Mathews & Schramm (1997) and Scully et al. (1997). This, in turn, could as well provide a convincing case for the evidently hot, massive, and considerably metal-enriched intragroup or intracluster gas components.

During the subsequent evolution many of the thick-disk degenerates could have become as faint as $M_V \sim 20$ for $\tau \sim 12$ Gyr (Hansen 1998, Chabrier 1999). Hence these "black dwarfs" can reach $V \sim 22$ mag at a mere 25 pc, and consequently any direct star counts – even nearby – could suffer from contaminant galaxies and subdwarfs. Nevertheless very deep exposures with a sufficient time baseline are a good means to search and discriminate for extremely faint nearby proper motion objects. A good example in this respect is the serendipitous detection of a very cool white dwarf at $V \sim 19$ mag by Hambly, Smartt & Hodgkin (1997). According to Hambly et al. (1999) this is a nearby object at a distance of 28 ± 4 pc and an absolute visual magnitude $M_V = 16.8 \pm 0.3$ mag. In the absence of any spectral lines in the observed spectrum its radial velocity is unknown. Yet, the measured transverse velocity (which translates to U/V/W= $-3/-154/-55$ km s^{-1}) implies a thick-disk status with reference to our results in the Toomre diagram of Fig. 17. As another example, even fainter white dwarf candidates have very recently been discussed by Scholz et al. (2000) in a new high-proper-motion survey in the southern sky. Perhaps the most intriguing case, however, is the recent finding of extremely faint high-proper-motion objects in the Hubble Deep Fields (north and south) by Ibata et al. (1999) and Méndez & Minniti (2000) and their interpretation as ancient, *blue* (as suggested by Hansen 1998) halo white dwarfs. For an alternative interpretation of the data, we notice however that the derived distance estimates to the stars in the sampled regions clearly favour a thick-disk origin.

As already mentioned above, our star count analysis of the previous subsection implies that *more* than ∼17% of the local white dwarfs must belong to the thick disk. Since a whole sequence of cooling ages is principally expected for these thick-disk stars, at least part of them should be readily identifiable. As the primary criterion for the population membership of the white dwarfs must come from the stars' kinematics, a major drawback however is that many radial velocities are not known, and if, are gravitationally redshifted by several tens of kilometers (the exact value of which is not known a priori). Therefore we follow the conservative approach of

Table 6. High-velocity white dwarfs in the sample of Sion et al. (1988). $\mathrm{N_{disk}}$ is the number of disk white dwarfs after exclusion of putative halo objects, with a transverse velocity T~ 150 km s^{-1} as a likely threshold value. The last three columns give the fractions of these disk stars with T >100, 85 and 70 km s^{-1}, respectively

Sp. Type	$\mathrm{N_{tot}}$	$\mathrm{N_{disk}}$	$\mathrm{N_{disk}}$ (T>100)	$\mathrm{N_{disk}}$ (T>85)	$\mathrm{N_{disk}}$ (T>70)
DA	421	409	22 (5.4%)	45 (11.0%)	86 (21.0%)
DB	53	51	2 (3.9%)	5 (9.8%)	13 (25.5%)
DC	88	78	13 (16.7%)	24 (30.8%)	32 (41.0%)
DQ	26	23	3 (13.0%)	3 (13.0%)	5 (21.7%)
DZ	25	25	1 (4.0%)	5 (20.0%)	6 (24.0%)
Σ	613	586	41 (7.0%)	82 (14.0%)	142 (24.2%)

Sion et al. (1988) neglecting radial-velocity data to derive tangential space motions. In Table 6 we present from the data of Sion et al. the various subgroups DA, DB, DC, DQ, and DZ, and give the relative fraction of disk stars as a function of T = $(\mathrm{U}^2+\mathrm{V}^2+\mathrm{W}^2)^{1/2} = 4.74\ \mu/\pi''$, the total tangential space velocity with respect to the Sun. With reference to our Fig. 17, in which all but one thick-disk members are found in the range 85 km s^{-1} $< v_{pec} <$ 180 km s^{-1} and keeping in mind that T is necessarily low-velocity biased, we designate stars with T > 150 km s^{-1} as halo candidates, and, likewise, adopt T > 70 km s^{-1} as a lower limit for thick-disk stars. For the reader's convenience we also tabulate star counts for T > 85 km s^{-1} and T > 100 km s^{-1} threshold values.

Inspection of Table 6 now implies that, while the local budget of white dwarfs is likely dominated by thin-disk members, there is also a fair amount of nearby thick-disk white dwarf candidates. This is particularly true for the DC white dwarfs.

Another, more recent, white dwarf sample of interest is that of Knox, Hawkins & Hambly (1999) of the ESO/SERC field 287, wherein the authors identify objects down to $B \sim 22.5$ mag. Their sample of 58 white dwarfs (which may in fact be a complete survey) reveals a *majority* (~ 55%) of disk stars with 70 km s^{-1} $<$ T < 150 km s^{-1}. Of course, a large fraction of them, as well as for the Sion et al. (1988) sample in Table 6, resides in the crucial interval 70 km s^{-1} $<$ T $<$ 85 km s^{-1}. We reiterate however that in both cases we are dealing with low-velocity-biased data, and at least HD 37124 of our sample reminds us that some thick-disk stars can reveal *total* space velocities as low as ∼70 km s^{-1}.

Thus, while it has been realized since long (Eggen & Greenstein 1967, Greenstein 1976, Sion & Liebert 1977) that the local white dwarfs are predominantly members of the "old" disk population, we identify now part of this as the thick disk.

Table 7. Thick-disk white dwarf candidates within 25 pc in the fourth edition of the Villanova *Catalog of Spectroscopically Identified White Dwarfs* (McCook & Sion 1999). Effective temperatures refer to Leggett, Ruiz & Bergeron (1998), Bergeron, Ruiz & Leggett (1997), and Sion et al. (1988) in that order of preference. In columns (9) through (12) "T" is the total tangential space velocity, "U, V, W" its respective tangential components. Note that the well-known Wolf 219 = WD 0341+182 is among the thick-disk candidates

(1) WD	(2) GJ	(3) LHS	(4) Giclas	(5) V [mag]	(6) M_V [mag]	(7) Sp. Type	(8) T_{eff} [K]	(9) U [km/s]	(10) V [km/s]	(11) W [km/s]	(12) T [km/s]
WD 0208+396	GJ 1042	LHS 151	G 74-7	14.51	13.39	DAZ7	7318	–39	–57	–25	73
WD 0213+427	GJ 91.3	LHS 153	G 134-22	16.22	14.68	DA9	5475	–46	–69	–17	85
WD 0255–705	GJ 2028	LHS 1474		14.08	12.23	DA6	10147	–25	–46	46	70
WD 0341+182	GJ 151	LHS 179	G 6-30	15.19	13.80	DQ8	6862	14	–94	–32	100
WD 0423+044	GJ 3288	LHS 1670		17.14	15.03	DC9	5136	15	–87	25	92
WD 0644+375	GJ 246	LHS 1870	G 87-7	12.10	10.59	DA2	19799	66	–46	–25	84
WD 0747+073A	GJ 1102B	LHS 239		16.96	15.65	DC9	4166	78	–129	–45	157
WD 0747+073B	GJ 1102A	LHS 240		16.63	15.32	DC9	4871	73	–118	–39	145
WD 1043–188		LHS 290		15.52	15.40	DQ9	6220	–64	–45	–72	107
WD 1247+550	GJ 3754	LHS 342		17.79	15.77	DC9	4000	101	–83	–49	140
WD 1327–083	GJ 515	LHS 354	G 14-58	12.31	11.92	DA3.5	10678	–59	–90	–1	108
WD 1334+039	GJ 518	LHS 46	G 62-53	14.63	15.05	DZ9	5048	–79	–113	14	138
WD 2251–070	GJ 1276	LHS 69		15.71	16.17	DZ9	4586	–58	–43	–44	84

We mention that this has also been suggested by J. Liebert as early as 1988 in a private communication to Sion et al. (1988).

A more quantitative assertion of what we can present in Table 6 has to await larger samples of F/G thick-disk stars to learn more about their kinematics. Then it is also necessary to have the full, i.e. radial-velocity-based, UVW data available. We also need deeper, as well as proper-motion-unbiased star counts of white dwarfs.[8] The recent large compilation of spectroscopically identified white dwarfs by McCook & Sion (1999), for instance, contains 2249 entries. Yet, while there are 23 white dwarfs within 10 pc tabulated, only 147 are known out to 25 pc, less than 50% of what one would expect. But also within 10 pc, a region with 400 odd stars, the registered inventory of white dwarfs is certainly not complete. From the McCook & Sion sample of white dwarfs within 25 pc and with reference to the velocity distribution of our identified F/G/K thick-disk stars we present – only meant as a rough guideline – a subset of 13 rather bright thick-disk candidates (on the base of their transverse velocities) in Table 7.

There are many studies in the literature that are concerned with the white dwarf luminosity function in an attempt to constrain the age of "the disk", "the Galaxy", or even "the Universe" (e.g. Weidemann 1967, Sion & Liebert 1977, Winget et al. 1987, Liebert, Dahn & Monet 1988, Evans 1992, Oswalt et al. 1995, Leggett, Ruiz & Bergeron 1998, Knox, Hawkins & Hambly 1999). From our analysis it is clear that what has been constrained is at best the age of the local thin disk. Among the many difficulties with the interpretation of the luminosity function, such as uncertain bolometric corrections for the faint white dwarfs, effects of core composition and chemical profile, delay of cooling via core crystallization and phase separation[9], as well as the different atmospheric transparencies (hydrogen vs helium composition), or the notorious low-number statistics at the faint end of the luminosity function, we may also notice that contaminant thick-disk white dwarfs have an impact as well. Thus the majority of the candidate thick-disk stars of Table 7 are also members of the often used "LDM" white dwarf sample (N=43) of Liebert, Dahn & Monet (1988) and consequently a correct interpretation of what is "observed" when analyzing the white dwarf cooling sequence requires a clean sample of stars. (Note that the LDM sample contains a few halo white dwarfs as well.) Future applications should account for these facts and it seems that work in this direction is indeed in progress (cf. Liebert et al. 1999, for a preliminary report). Again, what is badly needed, is a better understanding of the kinematics of the white dwarfs.

One point is also important to realize at this stage: while many thick-disk white dwarfs that we claim to exist are hard to detect – even nearby, an invariant initial mass function for the thick-disk population does not necessarily double the census of all types of disk stars. This is particularly true for the many K and M main-sequence stars in the immediate solar neighborhood. Herein it would, of course, only be the perspective that changes, the classification of the known objects, not their absolute number.

[8] recall that a high proper motion is a bias in favour of the thick-disk white dwarfs; on the other hand, some of them may have escaped detection because they are very faint

[9] contrary to the metal-poor stellar remnants of the Galactic halo, thick-disk white dwarfs should be more prone to the effects of the trace species Ne and Fe at solidification, as described in Segretain et al. (1994) and Hernanz et al. (1994)

Table 8. Kinematics and metallicities of all stars with accepted analyses (top) and those within 25 pc and $T_{eff} \geq 5400$ K on the main sequence (bottom). A circular speed of the local standard of rest of 220 km s^{-1} is adopted. The basic solar motion is taken from Dehnen & Binney (1998). "Young disk" and "old disk" refer to the stars of the thin disk, below and above ages of $\sim$4 Gyr, respectively. (To improve the data on the thick-disk kinematics, a row labeled " Thick Disk* " is appended which includes the giant Arcturus (taken as single), the blue straggler candidate HR 4657, and the chromospherically active star HD 165401)

(1) Population	(2) N	(3) U [km/s]	(4) σ_U [km/s]	(5) V [km/s]	(6) σ_V [km/s]	(7) W [km/s]	(8) σ_W [km/s]	(9) V_{rot} [km/s]	(10) [Fe/H] [dex]	(11) $\sigma_{\rm [Fe/H]}$ [dex]	(12) [Mg/H] [dex]	(13) $\sigma_{\rm [Mg/H]}$ [dex]
Young Disk	28	1	32	–9	14	–3	11	211	0.037	0.16	0.064	0.15
Old Disk	45	6	38	–16	19	–5	20	204	–0.060	0.23	–0.008	0.17
Thin Disk	73	4	36	–13	18	–4	17	207	–0.023	0.21	0.019	0.17
Transition	3	47	17	–55	30	28	1	165	–0.247	0.08	–0.037	0.08
Thick Disk	14	–29	58	–100	34	–7	44	120	–0.588	0.22	–0.210	0.21
Thick Disk*	17	–22	59	–98	32	–11	41	122	—	—	—	—
Halo	5	78	222	–191	61	–25	24	29	–1.602	0.40	–1.250	0.35
Young Disk	22	1	33	–9	14	–4	12	211	0.005	0.12	0.034	0.11
Old Disk	36	5	37	–16	19	–7	20	204	–0.037	0.22	0.009	0.17
Thin Disk	58	3	35	–14	18	–6	17	206	–0.021	0.19	0.018	0.15
Transition	2	48	23	–60	41	29	1	160	–0.285	0.06	–0.075	0.05
Thick Disk	3	–41	70	–77	3	–38	18	143	–0.493	0.32	–0.113	0.27
Thick Disk*	6	–16	68	–83	16	–33	23	137	—	—	—	—

Another point that we should briefly address is: what is the role played by the halo population(s) for the Galactic scenario? This is particularly legitimate to ask, inasmuch as the stars of the thick disk presumably dominate only up to $\sim$5 kpc above the Galactic plane (Majewski 1992), and the Milky Way halo region is of course much more extended (and thereby, in principal, another harbour for dim stellar remnants). As we have already argued in Paper I, our data suggest that the thick disk is not the result of a merger of the thin disk, but, instead, an ancient precursor population of the thin disk, the first "trial" or phase in the build-up of the disk structure. In this picture, and in particular with its ability to solve the well-known G-dwarf problem, we then have a rather straight explanation for the formation of the thin disk at our disposal. But, on the other hand, our data hardly address neither the origin of what was to become the thick disk nor that of the halo. Since (thick-)disk stars are generally more metal-rich than halo stars it has always been tempting to invoke a pre-existing halo population for the (thick) disk. There are, however, major drawbacks with this assumption. One is that star formation is an extremely non-linear process. As such, metal-rich stars can be very old, young stars in turn are not necessarily metal-rich. A real worrisome observation is also that a number of halo stars have been found in 1990s *without* Fe/α-element underabundances (e.g. Nissen & Schuster 1997). It is consequently not clear whether the thick-disk population (which presumably does not show this effect) is genuinely younger than "the halo". From the analysis of our (few) halo and thick-disk stars it appears that both are very old and also coeval, yet we notice very different kinematics. It is thus hard to image that a top-down evolution "halo – thick disk" took place in the early Galaxy. Instead, it seems more reasonable to follow Gilmore's (1995) suggestion that halo and thick disk have their own distinct evolutionary paths, the former to the bulge and the latter – as we have also argued above – to the thin disk.

5.5. Some more kinematics and chemistry

We now come back examining some additional aspects of the kinematics and chemistry of the analyzed stars, as summarized in Table 8. Herein, the upper part includes all 95 objects with reliable analyses (i.e. omitting spectroscopic binaries, chromospherically active stars, etc.). In the lower part the subset with d$\leq$25 pc and T_{eff} $\geq$5400 K on the main sequence is tabulated. This results in 63 stars. In both cases the stars of the thin disk are additionally resolved into "young" or "old" for ages below or above four billion years, respectively (note that this cut is at present an arbitrary choice). Thereby the "young" disk stars are found to have a mean age of $\sim$2.5 Gyr, whereas the "old" disk stars result in $\sim$6.5 Gyr; the average value for all thin-disk stars comes out with $\sim$5.0 Gyr. As explained in Sect. 3, the derived stellar ages are based upon, or interpolated within, existing evolutionary tracks from stellar interior calculations. Although some of these still require minor adjustments, this will have negligible consequences for the stars' *mean* properties. On the other hand, it is clear that our halo star sample cannot be statistically representative, and, of course, this also holds true for the presented thick-disk stars. The 58 thin-disk objects however represent by now a fraction of about 25% of our final volume-limited sample. Including the kinematics of *all* identified thin-disk objects of Tables 1, 3, and 5 as well as those of Paper I, increases this sample to 73 thin-disk stars, which corre-

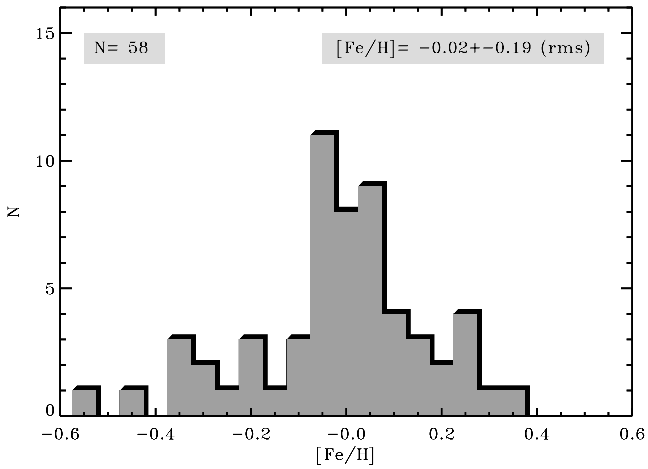

Fig. 20. Iron metallicity distribution function for the sample of 58 identified thin-disk F5 to G9 dwarf stars with $T_{eff} \geq 5400$ K on the main sequence and within 25 pc. The abscissa has been divided into 0.05 dex bins. The mean iron abundance is close to the *solar* value

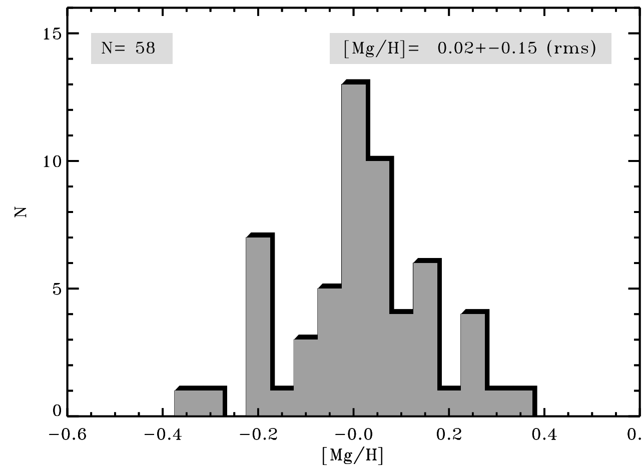

Fig. 21. Same as Fig. 21, but for magnesium abundances: again, the distribution peaks at a value not significantly different from *solar*

sponds to a 32% completeness. To derive the thin-disk velocity ellipsoid we exclude – with reference to Fig. 17 – the three outliers with $v_{pec} > 85$ km s^{-1}, namely, 31 Aql (which may in fact belong to the *bulge* population), HD 152391, and 5 Ser. This yields mean space velocities and velocity dispersions for the thin disk (N=70) as follows:

$$(U, V, W) = (6, -12, -4) \text{ km s}^{-1}$$
$$(\sigma_U, \sigma_V, \sigma_W) = (31, 18, 17) \text{ km s}^{-1}$$

From inspection of Table 8 we mention a change in the asymmetric drift velocity from $\langle \Delta V_{rot} \rangle = -9$ km s^{-1} for the "young" thin disk to $\langle \Delta V_{rot} \rangle = -16$ km s^{-1} for the "old" thin disk. It is also interesting to see the vertical velocity dispersion σ_W to evolve from 12 to 20 km s^{-1} within 4 Gyr. A somewhat smaller value $\sigma_W \sim 17$ km s^{-1} has been found by Gómez et al. (1997) on the base of a much larger Hipparcos sample. The authors find in particular no dynamically significant evolution in the vertical velocity dispersion for stellar ages beyond $\tau \sim 5$ Gyr. For our (biased) sample of thick-disk stars (N=17) the vertical velocity dispersion is found to be $\sigma_{W,thick} \sim 40$ km s^{-1}, which is further evidence that this population is not the continuous extension to the old thin disk. Nevertheless, one may also conjecture that the thick disk was presumably not as "thick" at its time of formation.

In Figs. 17 and 18 of Wallerstein's (1962) early survey of nearby field stars it is remarkable to see – and his merit to have realized – that it is the α/Fe *abundance ratio* rather than the straight iron abundance that segregates the stars (populations) in the displayed UV planes. Thus to characterize a star chemically it does generally not suffice to think only in terms of [Fe/H] or [m/H], with "m" representing some kind of a mean metallicity. From the general picture that massive stars produce the bulk of the α-elements via SN II, whereas the iron-peak elements predominantly come from SN Ia's, it is good to have at least one α-element in addition to the classical iron for an abundance study (in fact, knowledge of the *relative* elemental abundance pattern is a must for the underlying model atmosphere in a detailed spectroscopic analysis). We already discussed at length the meaning of the Mg versus Fe abundances in Fig. 12. Here we consequently present *two* metallicity distribution functions in Figs. 20 and 21 for our 58 reliably analyzed CNS4 stars of the thin disk. We recall that up to now we are complete for only one-third of the final volume-limited sample, i.e. our results must be considered "preliminary" at present. Both distribution functions may also contain a minor selection effect, in that they consist of an equal number of F and G stars, whereas the final sample will evolve to N(F):N(G)≈1:2. On the other hand, this bias should not exceed one or two hundredths of a dex in [Fe/H], and even less for [Mg/H], since we register from Table 8 that there is only a very weak *age-metallicity relation* of 0.042 dex within 4 Gyr for the iron content of the thin disk, and only 0.025 dex/4 Gyr for magnesium. A linear extrapolation to the age of the thin disk (~ 9 Gyr) thereby results in a mere Δ[Fe/H]~ 0.1 dex and Δ[Mg/H]~ 0.06 dex. This is an increase of about 20% for the Galactic iron content, and a minor $\sim$ 12% for the α-element magnesium in the evolution of the thin disk. As a result, we have not applied any disk evaporation correction factors (cf. Rana 1991, Sommer-Larsen 1991) for the metal-poor stars, as others have done (e.g. Rocha-Pinto & Maciel 1996, Favata, Micela & Sciortino 1997) for their metallicity distribution functions.[10] Along with the earlier finding that our abundance determinations are often slightly higher by Δ[Fe/H]~ 0.1 dex than many others (cf. Paper I), this leads to metallicity distribution functions for the thin disk that are close to *solar* for the mean values of both, Fe and Mg. As is also illus-

[10] disk heating affects the relative composition of the tracer populations, which is described by their various scale heights and normalization. The lack of a clear age-metallicity relation for the thin disk, in turn, causes an almost negligible effect on its metallicity distribution functions, provided one can identify the intruders of the thick disk and halo, as we do here

trated in Fig. 12, the abundance scale for magnesium is more compressed with a dispersion of $\sigma_{\rm [Mg/H]}$=0.15 dex, which is compared to $\sigma_{\rm [Fe/H]}$=0.19 dex for iron.

We conclude this subsection with a few remarks on the transition phase from thick disk to thin disk. If the aforementioned *weak* age-metallicity relations also hold for the complete thin-disk sample, this entails that the bulk of the iron production, starting at $\langle$ [Fe/H] $\rangle = -0.59$ for the thick disk, must have been extremely efficient within the suggested ∼3 Gyr star formation gap. That is, again, a considerable number of white dwarfs, part of which became SN Ia's, must have contributed early on. (In an extreme scenario one might even conjecture that it were the SN Ia's in that phase of evolution which gave rise to the star formation gap.) It also appears that with a mean $\langle$ [Mg/H] $\rangle = -0.21$ for the thick disk, and a mere ~ 0.06 dex increase during the subsequent thin-disk epoch, a major release of Mg (and Fe) *may* have taken place at the onset of the thin disk. A more quantitative assertion of this important point must however await a more robust data base.

6. Conclusions

As we have seen in the preceding sections, the study of nearby stars has far-reaching consequences for our notions of galactic astronomy. There is now a very good case for an *individual* identification of the stars from the thick disk and the thin disk, as well as their separation from the halo populations. Thus we expect a dozen of luminous (here: $T_{eff} \geq 5400$ K on the main sequence) thick-disk stars within 25 pc and north of $\delta = -15^{\rm o}$, which is only about 4% of the local budget of F, G, and evolved K stars.

Combining the thick-disk stars that we have up to now identified in this volume with the few kinematically *bona fide* candidates subject to forthcoming spectroscopic analyses, it is very likely that this *local*, small, but volume-complete, thick-disk sample will finally come out with an asymmetric Strömberg drift velocity $\langle \Delta V_{rot} \rangle \sim -80$ km s^{-1} with respect to the local standard of rest. Though this would be a slightly higher value than the $\langle \Delta V_{rot} \rangle \sim -100$ km s^{-1} that we could present herein from our (biased) sample of thick-disk stars, it nevertheless clearly demonstrates that the latter are kinematically fairly distinct from the thin-disk stars. We have given similar evidence for this finding from the vertical velocity dispersion, from the chemistry of the disk stars, and, most important, we suggest an age gap between the thick disk ($\tau_{min} \sim 12$ Gyr) and the thin disk ($\tau_{max} \sim 9$ Gyr), with the thick-disk population representing the precursor to the thin disk.

Our star-count analysis of long-lived stars readily leads to a picture of a high star-formation rate in the early "thick-disk epoch" of the Milky Way Galaxy. For the physics of galaxy formation, the Galactic thick disk (and, perhaps, the "classical" halo as well) may thus be the prototype of a component, wherein the luminosity is fairly *decoupled* from the mass, in that our *current* epoch renders a detection of this ancient population rather difficult, in spite of the possibility that the thick disk may be as massive as the thin disk. Although the latter suggestion is perhaps not tenable as a result of a possible mass cut at $M \sim 0.7 M_\odot$ for thick-disk stars, our data nevertheless imply the existence of tens of billions of thick-disk white dwarfs in the Galactic backyard, in particular, in the appealing case of a bimodal initial mass function for the disk populations. In the sense of *et respice finem* is then "*Dark matter – Dead stars?* ", as Larson asked in 1987, the valid scenario for (not only) the Milky Way? No doubt, part of the story must be in that direction and certainly our data impart profound bearings on the observed compact massive halo objects, as well as the study of high-redshift galaxies in general.

Thus, the "intermediate" population of the Milky Way that was in the air since at least the Vatican Conference in 1957, and then became popular by Gilmore & Reid in the early eighties, is perhaps best characterized as what one might call an "undercover population" or "the dark side of the disk", that, however, was – and is – very influential on what is recorded in the kinematics and chemistry of the ubiquitous forest of foreground thin-disk stars. The formerly troublesome G-dwarf problem is just another example in this respect. The more embarrassing case, however, is that the dark part of the thick disk may in fact account for the observed light disk to be rotationally supported from ordinary baryonic matter alone, for perhaps not only the inner Milky Way.

Hence, while one could read a decade ago in the textbook of Binney & Tremaine (1987) that "*roughly a third of material in the solar neighborhood must be considered to be dark matter*", an assertion that is obviously outdated from the robust Hipparcos astrometry (cf. Crézé et al. 1998), we may now also learn from the stellar remnants, and supporting Sackett's (1997) provocative question, that the Galactic disk is not as submaximal as generally thought. Likewise, the recently announced detection of large-scale molecular hydrogen in the disk of NGC 891 (the "Milky Way edge-on") by Valentijn & van der Werf (1999, and references therein) gives further evidence for baryonic-matter-dominated rotation curves. It also appears that adopting a local Galactic escape velocity of ∼450...650 km s^{-1} (see Leonard & Tremaine 1990) for extreme halo stars to probe the mass of the Galaxy is not realistic. This is because there are now a couple of intriguing findings that point to *accretion* as a major phenomenon and a *multi-component* Galactic halo (e.g. Ibata, Gilmore & Irwin 1994, Johnston 1999, Majewski 1999, and references therein). In other words, as a number of halo stars have also been found to lack the usual Fe/α underabundance (cf. Carney & Latham 1985, Nissen & Schuster 1997, King 1997, Laird 1999, Carney 1999, and references therein) and some of these show very extreme space velocities, it could well be that they represent interlopers, only bound to the Local Group of galaxies, and that $v_{esc} \sim 400$ km s^{-1} (which may be also a lower limit to the Hipparcos data, according to Meillon et al. 1997) is presumably more appropriate for the "classical" Milky Way halo stars.

In summary, it thus seems prudent not to forget that, no doubt, dark matter dominates the most, where our knowledge of the expected deposits is frankly the least, namely, at large distances. But if there are as many things to learn with the help of a 29 cm astrometry satellite telescope that was predominantly dedicated to explore the *immediate* solar neighborhood, what can be learnt on the kiloparsec scales in focus of the ambitious mission successors like DIVA, FAME, or GAIA in the decades to come.

Acknowledgements. It's a pleasure to thank U. Bastian, J. Bernkopf, A. Fiedler, T. Gehren, R. Giacconi, F. Grupp, H. Jahreiß, A. Korn, R. Kudritzki, L. Mashonkina, L. Pasquini, S. Pedraz, M.J. Pfeiffer, J. Shi, D. VandenBerg, C. van't Veer-Menneret, R. Wielen, and G. Zhao for help and valuable discussions. I am very grateful to B. Barbuy, G. and R. Cayrel, B. Fuchs, B. Gustafsson, P.E. Nissen and B. Pagel for their generous support. I also acknowledge financial support from a number of travel grants from ESO and DFG (the latter under Fu 198/5-1 through 7-1 and Fu 198/9-1) to the Paranal and Calar Alto Observatories in 1998 and 1999. The most recent run at Calar Alto in January 2000 was realized by my dear wife Meike, who is also thanked for her continuous help within the last ∼18 months during which this research proceeded. A quest to the *Deutsche Forschungsgemeinschaft, DFG*, in February 1999 for a research grant on the base of the results of Paper I was instantaneously and generously rejected by the end of that year. Even after pre-submitting the current results in front of the reader and an explicit undertaking towards the *Deutsche Forschungsgemeinschaft* (and its competent german referees) to *realize* that "some" people are indeed interested in this work, there was no response. Evidently, this seems characteristic for the inflexibility and early solidification in the specific phase diagram of this large-scale organization (cf. also M. Benecke, "DFG – die Entdeckung der Langsamkeit", SZ, 1. Feb. 2000). Since there is the claim by the *Deutsche Forschungsgemeinschaft* – in fact the legitimacy for its existence – *"to serve science and the arts in all fields by supporting research projects carried out in universities and public research institutions in Germany"* their negative decision for this project certainly comes as a real mystery, perhaps somewhat reminiscent of the putative dark matter around us. But note, there is at least some hope that we may understand the latter some day.

References

Abt, H.A., Levy, S.G., 1976, ApJS 30, 273
Alcock, C., Allsman, R.A., Alves, D., et al., 1997, ApJ 486, 697
Alonso, A., Arribas, S., Martínez-Roger, C., 1995, A&A 297, 197
Anderson, K.S., Kraft, R.P., 1972, ApJ 172, 631
Baize, P., 1976, A&AS 26, 177
Baliunas, S.L., Donahue, R.A., Soon, W.H., et al., 1995, ApJ 438, 269
Beers, T.C., Sommer-Larsen, J., 1995, ApJS 96, 175
Bergeron, P., Ruiz, M.T., Leggett, S.K., 1997, ApJS 108, 339
Bernkopf, J., 1998, A&A 332, 127
Binney, J., Tremaine, S., 1987, *Galactic Dynamics*, Princeton University Press
Burleigh, M.R., Barstow, M.A., Fleming, T.A., 1997, MNRAS 287, 381
Carney, B.W., 1999, ASP Conf. Ser. 165, 230
Carney, B.W., Latham, D.W., 1985, AJ 298, 803
Carney, B.W., Latham, D.W., Laird, J.B., 1989, AJ 97, 423
Carney, B.W., Laird, J.B., Latham, D.W., et al., 1996, AJ 112, 668
Cayrel de Strobel, G., 1996, A&AR 7, 243
Chabrier, G., 1999, ApJ 513, L103
Chabrier, G., Segretain, L., Méra, D., 1996, ApJ 468, L21
Chen, Y.Q., Nissen, P.E., Zhao, G., et al., 2000, A&AS 141, 491
Chmielewski, Y., Cayrel de Strobel, G., Cayrel, R., et al., 1995, A&A 299, 809
Crézé, M., Chereul, E., Bienaymé, O., et al., 1998, A&A 329, 920
Dehnen, W., Binney, J.J., 1998, MNRAS 298, 387
Donahue, R.A., Saar, S.H., Baliunas, S.L., 1996, ApJ 466, 384
Dravins, D., Lindegren, L., VandenBerg, D.A., 1998, A&A 330, 1077
Duquennoy, A., Mayor, M., 1991, A&A 248, 485
Edvardsson, B., 1988, A&A 190, 148
Edvardsson, B., Andersen, J., Gustafsson, B., et al., 1993, A&A 275, 101
Eggen, O.J., 1971, PASP 83, 271
Eggen, O.J., 1998a, AJ 115, 2397
Eggen, O.J., 1998b, AJ 115, 2435
Eggen, O.J., Greenstein, J.L., 1967, ApJ 150, 927
Evans, D.W., 1992, MNRAS 255, 521
Favata, F., Micela, G., Sciortino, S., 1997, A&A 323, 809
Fields, B.D., Mathews, G.J., Schramm, D.N., 1997, ApJ 483, 625
Flynn, C., Morell, O., 1997, MNRAS 286, 617
Fuhrmann, K., 1998, A&A 338, 161
Fuhrmann, K., Bernkopf, J., 1999, A&A 347, 897
Gehren, T., 1975, *LTE-Sternatmosphärenmodelle*, Kiel
Gilmore, G., 1995, IAU Symp. 164, 99
Gilmore, G., Reid, N., 1983, MNRAS 202, 1025
Gómez, A.E., Grenier, S., Udry, S., et al., 1997, ESA SP-402, p. 621
Graff, D.S., Laughlin, G., Freese, K., 1998, ApJ 499, 7
Gray, D.F., 1977, ApJ 218, 530
Gray, D.F., 1984, ApJ 281, 719
Gray, D.F., 1992, *The observation and analysis of stellar photospheres*, Cambridge University Press
Greenstein, J.L., 1976, AJ 81, 323
Grenon, M., 1999, Ap&SS 265, 331
Griffin, R.F., 1998, Obs 118, 299
Hambly, N.C., Smartt, S.J., Hodgkin, S.T., 1997, ApJ 489, L157
Hambly, N.C., Smartt, S.J., Hodgkin, S.T., et al., 1999, MNRAS 309, L33
Hansen, B.M.S., 1998, Nat 394, 860
Hartkopf, W.I., McAlister, H.A., 1984, PASP 96, 105
Haywood, M., Palasi, J., Gómez, A., et al., 1997, ESA SP-402, p. 489
Herbig, G.H., 1985, ApJ 289, 269
Hernanz, M., García-Berro, E., Isern, J., et al., 1994, ApJ 434, 652
Ibata, R.A., Gilmore, G., Irwin, M., 1994, Nat 370, 194
Ibata, R.A., Richer, H.B., Gilliland, R.L., et al., 1999, ApJ 524, L95
Jahreiß, H., Fuchs, B., Wielen, R., 1997, ESA SP-402, p. 587
Jahreiß, H., Wielen, R., 1997, ESA SP-402, p. 675
Johnston, K.V., 1999, ASP Conf. Ser. 165, 64
King, J.R., 1997, AJ 113, 2302
Knox, R.A., Hawkins, M.R.S., Hambly, N.C., 1999, MNRAS 306, 736
Kraft, R.P., 1967, ApJ 150, 551
Kroupa, P., Tout, C.A., Gilmore, G., 1993, MNRAS 262, 545
Kuijken, K., 1995, IAU Symp. 164, 195
Kurucz, R.L., Furenlid, I., Brault, J., Testerman, L., 1984, *Solar Flux Atlas from 296 to 1300 nm*, KPNO, Tucson
LaBonte, B.J., 1986, ApJS 62, 241
Laird, J.B., 1999, ASP Conf. Ser. 165, 248
Larson, R.B., 1986, MNRAS 218, 409
Larson, R.B., 1987, ComAp 11, 273
Leggett, S.K., Ruiz, M.T., Bergeron, P., 1998, ApJ 497, 294
Leonard, P.J.T., Tremaine, S., 1990, ApJ 353, 486
Liebert, J., Dahn, C.C., Monet, D.G., 1988, ApJ 332, 891
Liebert, J., Dahn, C.C., Harris, H.C., et al., 1999, ASP Conf. Ser. 169, 51

Majewski, S.R., 1992, ApJS 78, 87
Majewski, S.R., 1999, ASP Conf. Ser. 165, 76
McCook, G.P., Sion, E.M., 1999, ApJS 121, 1
Meillon, L., Crifo, F., Gómez, A., et al., 1997, ESA SP-402, p. 591
Méndez, R.A., Minniti, D., 2000, ApJ 529, 911
Méra, D., Chabrier, G., Schaeffer, R., 1998, A&A 330, 953
Mermilliod, J.-C., Mermilliod, M., Hauck, B., 1997, A&AS 124, 349
Montesinos, B., Jordan, C., 1993, MNRAS 264, 900
Morbey, C.L., Griffin, R.F., 1987, ApJ 317, 343
Nissen, P.E., Schuster, W.J., 1997, A&A 326, 751
Norris, J.E., 1999, Ap&SS 265, 213
Ojha, D.K., Bienaymé, O., Robin, A.C., et al., 1994, A&A 290, 771
Ojha, D.K., Bienaymé, O., Robin, A.C., et al., 1996, A&A 311, 456
Oswalt, T.D., Smith, J.A., Wood, M.A., et al., 1995, Nat 382, 692
Pagel, B.E.J., Patchett, B.E., 1975, MNRAS 172, 13
Pfeiffer, M.J., Frank, C., Baumüller, D., et al., 1998, A&AS 130, 381
Pham, H.A., 1997, ESA SP-402, p. 559
Porto de Mello, G.F., da Silva, L., 1997, ApJ 482, L89
Pounds, K.A., Allan, D.J., Barber, C., et al., 1993, MNRAS 260, 77
Radick, R.R., Lockwood, G.W., Skiff, B.A., et al., 1998, ApJS 118, 239
Rana, N.C., 1991, ARA&A 29, 129
Rocha-Pinto, H.J., Maciel, W.J., 1996, MNRAS 279, 447
Saar, S.H., Osten, R.A., 1997, MNRAS 284, 803
Sackett, P.D., 1997, ApJ 483, 103
Sandage, A., Fouts, G., 1987, AJ 93, 74
Scholz, R.-D., Irwin, M., Ibata, R., et al., 2000, A&A 353, 958
Schuster, W.J., Nissen, P.E., 1989, A&A 221, 65
Schuster, W.J., Parrao, L., Contreras Martínez, M.E., 1993, A&AS 97, 951
Schwarzschild, M., Spitzer, L., 1953, Obs 73, 77
Scully, S., Cassé, M., Olive, K.A., et al., 1997, ApJ 476, 521
Segretain, L., Chabrier, G., Hernanz, M., et al., 1994, ApJ 434, 641
Sion, E.M., Liebert, J., 1977, ApJ 213, 468
Sion, E.M., Fritz, M.L., McMullin, J.P., et al., 1988, AJ 96, 251
Skuljan, J., Cottrell, P.L., Hearnshaw, J.B., 1997, ESA SP-402, p. 525
Smith, G.H., Churchill, C.W., 1998, MNRAS 297, 388
Soderblom, D.R., 1985, AJ 90, 2103
Soderblom, D.R., 1990, AJ 100, 204
Soderblom, D.R., Duncan, D.K., Johnson, D.R., 1991, ApJ 375, 722
Sommer-Larsen, J., 1991, MNRAS 249, 368
Soubiran, C., 1993, A&A 274, 181
Tamanaha, C.M., Silk, J., Wood, M.A., et al., 1990, ApJ 358, 164
Valentijn, E.A., van der Werf, P.P., 1999, ApJ 522, L29
VandenBerg, D.A., Swenson, F.J., Rogers, F.J., et al., 2000, ApJ 532, 430
van den Bergh, S., 1962, AJ 67, 486
Wallerstein, G., 1962, ApJS 6, 407
Weidemann, V., 1967, ZfA 67, 286
Winget, D.E., Hansen, C.J., Liebert, J., et al., 1987, ApJ 315, L77
Wyse, R.F.G., Gilmore, G., 1986, AJ 91, 855
Wyse, R.F.G., Gilmore, G., 1995, AJ 110, 2771